Chapter 13

J. MICHAEL DUNCAN

SOIL SLOPE STABILITY ANALYSIS

Analyses of slopes can be divided into two categories: those used to evaluate the stability of slopes and those used to estimate slope movement. Although stability and movement are closely related, two different and distinct types of analyses are almost always used to evaluate them.

1. INTRODUCTION

Stability of slopes is usually analyzed by methods of limit equilibrium. These analyses require information about the strength of the soil, but do not require information about its stress-strain behavior. They provide no information about the magnitude of movements of the slope.

Movements of slopes are usually analyzed by the finite-element method. Understanding the stress-strain behavior of the soils is required for these analyses, and information regarding the strengths of the soils may also be required. Although these methods define movements and stresses throughout the slope, they do not provide a direct measure of stability, such as the factor of safety calculated by limit equilibrium analyses.

The focus in this chapter is on soil slopes and mechanisms involving shear failure within the soil mass. The methods described are applicable to landslides in weak rocks, where the location of the rupture surface is not controlled by existing discontinuities within the mass (see also Chapter 21). Analyses of slopes in strong rock, where instability mechanisms are controlled by existing discontinuities, are described in Chapter 15. Techniques for evaluating rock strength are discussed in Chapter 14, and those for evaluating soil strength are discussed in Chapter 12.

Limit equilibrium and finite-element analyses are described in subsequent sections of this chapter. Methods that are useful for practical purposes are emphasized, and their uses are illustrated by examples.

2. MECHANICS OF LIMIT EQUILIBRIUM ANALYSES

In limit equilibrium techniques, slope stability is analyzed by first computing the factor of safety. This value must be determined for the surface that is most likely to fail by sliding, the so-called *critical slip surface*. Iterative procedures are used, each involving the selection of a potential sliding mass, subdivision of this mass into a series of slices, and consideration of the equilibrium of each of these slices by one of several possible computational methods. These methods have varying degrees of computational accuracy depending on the suitability of the underlying simplifying assumptions for the situation being analyzed.

2.1 Factor of Safety

The factor of safety is defined as the ratio of the shear strength divided by the shear stress required for equilibrium of the slope:

$$F = \frac{\text{shear strength}}{\text{shear stress required for equilibrium}} \quad (13.1)$$

which can be expressed as

$$F = \frac{c + \sigma \tan\phi}{\tau_{eq}} \quad (13.2)$$

in which

F = factor of safety,
c = cohesion intercept on Mohr-Coulomb strength diagram,
ϕ = angle of internal friction of soil,
σ = normal stress on slip surface, and
τ_{eq} = shear stress required for equilibrium.

The cohesive and frictional components of strength (c and ϕ) are defined in Chapter 12.

The factor of safety defined by Equations 13.1 and 13.2 is an overall measure of the amount by which the strength of the soil would have to fall short of the values described by c and ϕ in order for the slope to fail. This strength-related definition of F is well suited for practical purposes because soil strength is usually the parameter that is most difficult to evaluate, and it usually involves considerable uncertainty.

In discussing equilibrium methods of analysis, it is sometimes said that the factor of safety is assumed to have the same value at all points on the slip surface. It is unlikely that this would ever be true for a real slope. Because the assumption is unlikely to be true, describing this assumption as one of the fundamental premises of limit equilibrium methods seems to cast doubt on their practicality and reliability. It is therefore important to understand that Equation 13.1 defines F, and it does not involve the assumption that F is the same at all points along the slip surface for a slope not at failure. Rather, F is the numerical answer to the question, By what factor would the strength have to be reduced to bring the slope to failure by sliding along a particular potential slip surface? The answer to this question can be determined reliably by limit equilibrium methods and is of considerable practical value.

To calculate a value of F as described above, a potential slip surface must be described. The slip surface is a mechanical idealization of the surface of rupture (see Chapter 3, Section 3.1 and Table 3-3). In general, each potential slip surface results in a different value of F. The smaller the value of F (the smaller the ratio of shear strength to shear stress required for equilibrium), the more likely failure is to occur by sliding along that surface. Of all possible slip surfaces, the one where sliding is most likely to occur is the one with the minimum value of F. This is the *critical slip surface*.

To evaluate the stability of a slope by limit equilibrium methods, it is necessary to perform calculations for a considerable number of possible slip surfaces in order to determine the location of the critical slip surface and the corresponding minimum value of F. This process is described as searching for the critical slip surface. It is an essential part of slope stability analyses.

2.2 Equations and Unknowns

All of the practically useful methods of analysis are methods of slices, so called because they subdivide the potential sliding mass into slices for purposes of analysis. Usually the slice boundaries are vertical, as shown in Figure 13-1. Two useful simplifications are achieved by subdividing the mass into slices:

1. The base of each slice passes through only one type of material, and
2. The slices are narrow enough that the segments of the slip surface at the base of each slice can be accurately represented by a straight line.

The equilibrium conditions can be considered slice by slice. If a condition of equilibrium is sat-

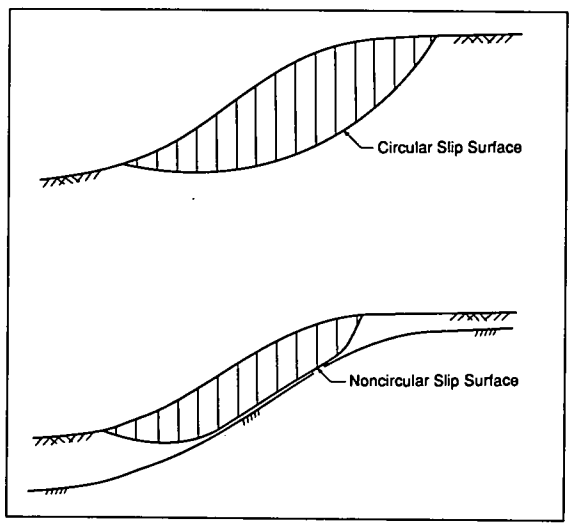

FIGURE 13-1 Division of potential sliding masses into slices (slip surface is idealization of surface of rupture; see Chapter 3, Section 3.1).

isfied for each and every slice, it is also satisfied for the entire mass. The forces on a slice are shown in Figure 13-2.

The number of equations of equilibrium available depends on the number of slices (N) and the number of equilibrium conditions that are used. As shown in Table 13-1, the number of equations available is $2N$ if only force equilibrium is to be satisfied and $3N$ if both force and moment equilibria are to be satisfied. If only force equilibrium is satisfied, the number of unknowns is $3N - 1$. If both force and moment equilibria are satisfied, the number of unknowns is $5N - 2$. In the special case in which $N = 1$, the problem is statically determinate, and the number of equilibrium equations is equal to the number of unknowns. To represent a slip surface with realistic shapes, it is usually necessary to use 10 to 40 slices, and the number of unknowns therefore exceeds the number of equations. The excess of unknowns over equations is $N - 1$ for force equilibrium analyses and $2N - 2$ for analyses that satisfy all conditions of equilibrium. Thus, such problems are statically indeterminate, and assumptions are required to make up the imbalance between equations and unknowns.

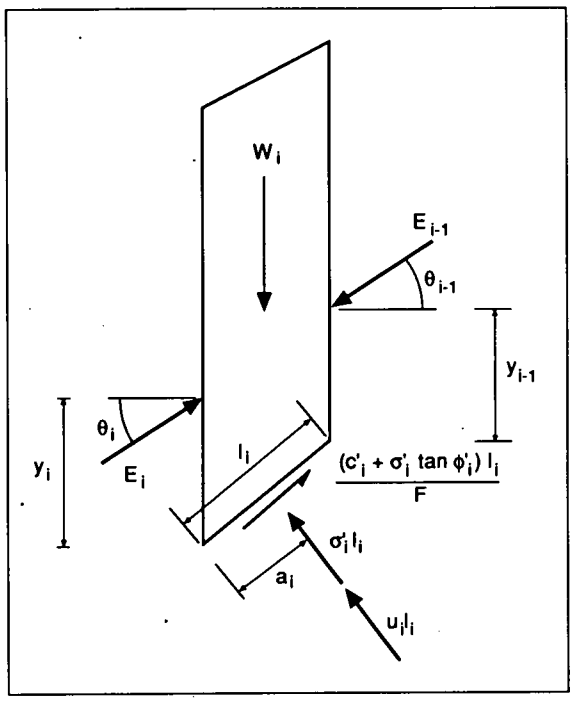

FIGURE 13-2
Forces on slice i.

2.3 Characteristics of Methods

The various methods of limit equilibrium analysis differ from each other in two regards:

1. Different methods use different assumptions to make up the balance between equations and unknowns, and
2. Some methods, such as the ordinary method of slices (Fellenius 1927) and Bishop's modified method (Bishop 1955), do not satisfy all conditions of equilibrium or even the conditions of force equilibrium.

Table 13-1
Equations and Unknowns in Limit Equilibrium Analysis of Slope Stability

EQUATIONS	UNKNOWNS
Methods That Satisfy Only Force Equilibrium	
N = horizontal equilibrium	N = normal forces on bases of slices
N = vertical equilibrium	$N - 1$ = side forces
	$N - 1$ = side force angles, θ
	1 = factor of safety
$2N$ total equations	$3N - 1$ total unknowns
Methods That Satisfy Both Force and Moment Equilibria	
N = horizontal equilibrium	N = normal forces on bases of slices
N = vertical equilibrium	N = locations of normal forces on bases
N = moment equilibrium	$N - 1$ = side forces
	$N - 1$ = side force angles, θ
	$N - 1$ = locations of side forces on slices
	1= factor of safety
$3N$ total equations	$5N - 2$ total unknowns

These methods therefore involve fewer equations and unknowns than those shown in Table 13-1. The characteristics of various practically used methods with regard to the conditions of equilibrium that they satisfy, the assumptions they involve, and their computational accuracies are summarized in Table 13-2.

2.4 Computational Accuracy

"Computational accuracy" here refers to the inherent accuracy with which the various methods handle the mechanics of slope stability and the limitations on accuracy that result from the fact that the equations of equilibrium are too few to solve for the factor of safety without using assumptions. The computational accuracy involves only the accuracy with which the shear stress required for equilibrium (τ_{eq}) and the normal stress σ can be evaluated. Computational accuracy is thus distinct from overall accuracy, which involves also the accuracy with which site conditions and shear strengths can be evaluated. By separating issues that determine computational accuracy from the other issues, it is possible to answer the following important questions:

1. Do any of the various limit equilibrium methods provide accurate values of F, and
2. How are the values of F affected by the assumptions involved in the various methods?

Table 13-2
Characteristics of Commonly Used Methods of Limit Equilibrium Analysis for Slope Stability

Method	Limitations, Assumptions, and Equilibrium Conditions Satisfied
Ordinary method of slices (Fellenius 1927)	Factors of safety low—very inaccurate for flat slopes with high pore pressures; only for circular slip surfaces; assumes that normal force on the base of each slice is $W \cos \alpha$; one equation (moment equilibrium of entire mass), one unknown (factor of safety)
Bishop's modified method (Bishop 1955)	Accurate method; only for circular slip surfaces; satisfies vertical equilibrium and overall moment equilibrium; assumes side forces on slices are horizontal; $N+1$ equations and unknowns
Force equilibrium methods (Section 6.1.3)	Satisfy force equilibrium; applicable to any shape of slip surface; assume side force inclinations, which may be the same for all slices or may vary from slice to slice; small side force inclinations result in values of F less than calculated using methods that satisfy all conditions of equilibrium; large inclinations result in values of F higher than calculated using methods that satisfy all conditions of equilibrium; $2N$ equations and unknowns
Janbu's simplified method (Janbu 1968)	Force equilibrium method; applicable to any shape of slip surface; assumes side forces are horizontal (same for all slices); factors of safety are usually considerably lower than calculated using methods that satisfy all conditions of equilibrium; $2N$ equations and unknowns
Modified Swedish method (U.S. Army Corps of Engineers 1970)	Force equilibrium method, applicable to any shape of slip surface; assumes side force inclinations are equal to the inclination of the slope (same for all slices); factors of safety are often considerably higher than calculated using methods that satisfy all conditions of equilibrium; $2N$ equations and unknowns
Lowe and Karafiath's method (Lowe and Karafiath 1960)	Generally most accurate of the force equilibrium methods; applicable to any shape of slip surface; assumes side force inclinations are average of slope surface and slip surface (varying from slice to slice); satisfies vertical and horizontal force equilibrium; $2N$ equations and unknowns
Janbu's generalized procedure of slices (Janbu 1968)	Satisfies all conditions of equilibrium; applicable to any shape of slip surface; assumes heights of side forces above base of slice (varying from slice to slice); more frequent numerical convergence problems than some other methods; accurate method; $3N$ equations and unknowns
Spencer's method (Spencer 1967)	Satisfies all conditions of equilibrium; applicable to any shape of slip surface; assumes that inclinations of side forces are the same for every slice; side force inclination is calculated in the process of solution so that all conditions of equilibrium are satisfied; accurate method; $3N$ equations and unknowns
Morgenstern and Price's method (Morgenstern and Price 1965)	Satisfies all conditions of equilibrium; applicable to any shape of slip surface; assumes that inclinations of side forces follow a prescribed pattern, called $f(x)$; side force inclinations can be the same or can vary from slice to slice; side force inclinations are calculated in the process of solution so that all conditions of equilibrium are satisfied; accurate method; $3N$ equations and unknowns
Sarma's method (Sarma 1973)	Satisfies all conditions of equilibrium; applicable to any shape of slip surface; assumes that magnitudes of vertical side forces follow prescribed patterns; calculates horizontal acceleration for barely stable equilibrium; by prefactoring strengths and iterating to find the value of the prefactor that results in zero horizontal acceleration for barely stable equilibrium, the value of the conventional factor of safety can be determined; $3N$ equations, $3N$ unknowns

Studies of computational accuracy have shown the following:

1. If the method of analysis satisfies all conditions of equilibrium, the factor of safety will be accurate within ±6 percent. This conclusion is based on the finding that factors of safety calculated using methods that satisfy all conditions of equilibrium never differ by more than 12 percent from each other or ±6 percent from a central value as long as the methods involve reasonable assumptions. The methods of Morgenstern and Price (1965), Spencer (1967), and Sarma (1973) and the generalized procedure of slices (GPS) (Janbu 1968) satisfy all conditions of equilibrium and involve reasonable assumptions. Studies have shown that values of F calculated using these methods differ by no more than 6 percent from values calculated using the log spiral method and the finite-element method, which satisfy all conditions of equilibrium but are not methods of slices.
2. Bishop's modified method is a special case. Although it does not satisfy all conditions of equilibrium, it is as accurate as methods that do. It is limited to circular slip surfaces.
3. No matter what method of analysis is used, it is essential to perform a thorough search for the critical slip surface to ensure that the minimum factor of safety has been calculated.

2.5 Checking Accuracy of Analyses

When slope stability analyses are performed, it is desirable to have an independent check of the results as a guard against mistakes. Unfortunately, computations using methods that satisfy all conditions of equilibrium are lengthy and complex, too involved for hand calculation. It is therefore more practical to use other, simpler types of analyses that can be performed by hand to check computer analyses.

When analyses are performed using circular slip surfaces, the factor of safety for the critical circle can be checked approximately by using the ordinary method of slices or Bishop's modified method. The ordinary method of slices gives values of F that are lower than values calculated by more accurate methods. For total stress analyses the difference is seldom more than 10 percent, but it may reach 50 percent for effective stress analyses under conditions involving high pore pressures. Bishop's modified method, only slightly more time-consuming than the ordinary method of slices, is as accurate as the methods that satisfy all conditions of equilibrium.

Charts provide a simple and effective means of checking slope stability analyses. Although approximations and simplifications are always necessary when charts are used, it is usually possible to calculate the factor of safety with sufficient accuracy to afford a useful check on the results of more detailed analyses. It is also useful to perform chart analyses before detailed computer analyses in order to get the best possible understanding of the problem.

When analyses are performed using noncircular slip surfaces, the results can be checked by hand for the critical slip surface using force equilibrium analyses. If Spencer's method is used for the computer analyses, the results for the critical slip surface can be checked by hand using force equilibrium analyses with the same side force inclination. If Morgenstern and Price's method or Janbu's GPS is used for the computer analyses, the force equilibrium hand calculations can be performed using an average side force inclination determined from the computer analyses.

Another means of checking computer analyses of slope stability is to perform independent analyses using another computer program and completely separate input. It is always desirable to have a different person perform the check analyses to make them as independent as possible.

3. DRAINED AND UNDRAINED CONDITIONS

Slope failures may occur under drained or undrained conditions in the soils that make up the slope. If instability is caused by changes in loading, such as removal of material from the bottom of the slope or increase in loads at the top, soils that have low values of permeability may not have time to drain during the length of time in which the loads are changed; thus they may contain unequalized excess pore pressures leading to slope failure. In that case, these low-permeability soils are said to be undrained. Under the same rates of loading, soils with higher permeabilities may have time to drain and will have no significant excess pore pressures.

One of the most important determinations needed for slope stability analyses is that of the

drainage conditions in the various soils that form the slope. A rational way of making this determination is to calculate the value of the dimensionless time factor T using the following equation:

$$T = \frac{C_v t}{D^2} \tag{13.3}$$

where

T = dimensionless time factor,
C_v = coefficient of consolidation (length squared per unit of time),
t = time for drainage to occur (units of time), and
D = length of drainage path (units of length).

D is the distance water would have to flow to drain from the soil zone. Usually D is defined as half the thickness of the soil layer or zone. If the soil zone is drained on only one side, D is equal to the thickness of the zone.

If the value of T is 3.0 or more, the soil zone will drain as rapidly as the loads are applied, and the soil within the zone can be treated as fully drained in the analysis. If the value of T is 0.01 or less, very little drainage will occur during the loading period, and the soil within the zone can be treated as completely undrained in the analysis. If the value of T is between 0.01 and 3.0, partial drainage will occur during the period of time when the loads are changing. In that case both drained and undrained conditions should be analyzed to bound the problem. For normal rates of loading, involving weeks or months, soils with permeabilities greater than 10^{-4} cm/sec are usually drained, and soils with permeabilities less than 10^{-7} cm/sec are usually undrained. Silts, which have permeabilities between 10^{-4} and 10^{-7} cm/sec, are often partially drained.

If instability in a slope is caused by increasing pore-water pressures *within* the slope, failure occurs under drained conditions by definition because adjustment of internal pore pressures in equilibrium with the flow boundary conditions is drainage. Changes in internal water pressures are often the cause of instability in natural slopes, where landslides almost always occur during wet periods. Such problems should be analyzed as drained conditions.

4. TOTAL STRESS AND EFFECTIVE STRESS ANALYSES

Stability of slopes can be analyzed using either effective stress or total stress methods:

- In effective stress analyses the shear strength of the soil is related to the effective normal stress on the potential slip surface by means of effective stress shear strength parameters. Pore pressures within the soil must be known and are part of the information required for analysis.
- In total stress analyses the shear strength of the soil is related to the total normal stress on the potential slip surface by means of total stress shear strength parameters. Pore pressures within the soil mass need not be known and are not required as input for analysis.

In principle, it is always possible to analyze stability by using effective stress methods because the strengths of soils are governed by effective stresses under both undrained and drained conditions. In practice, however, it is virtually impossible to determine accurately what excess pore pressures will result from changes in external loading on a slope (excavation, fill placement, or change in external water level). Because the excess pore pressures for these loading conditions cannot be estimated accurately, it is not possible to perform accurate analyses of stability for these conditions using effective stress procedures.

Total stress analyses for soils that do not drain during the loading period involve a simple principle: if an element of soil in the laboratory (a laboratory test specimen) is subjected to the same changes in stress under undrained conditions as an element of the same soil would experience in the field, the same excess pore pressures will develop. Thus, if the total stresses in the laboratory and the field are the same, the effective stresses will also be the same. Because soil strength is controlled by effective stresses, the strength measured in laboratory tests should be the same as the strength in the field if the pore pressures and total stresses are also the same. Thus, under undrained conditions, strengths can be related to total stresses, obviating the need to specify undrained excess pore pressures.

Although the principle outlined in the preceding paragraph is reasonably simple, experience has shown that many factors influence the pore pressures that develop under undrained loading. These factors include degree of saturation, density, stress history of the soil, rate of loading, and the magnitudes and orientations of the applied stresses. As a result, determining total stress-related undrained strengths by means of laboratory or in situ testing

is not a simple matter; considerable attention to detail is required if reliable results are to be achieved. Shear strengths for use in undrained total stress analyses must be measured using test specimens and loading conditions that closely duplicate the conditions in the field. Still, using total stress procedures for analysis of undrained conditions is more straightforward and more reliable than trying to predict undrained excess pore pressures for use in effective stress analyses of undrained conditions.

If a slope consists of soils of widely differing permeabilities, it is possible that the more permeable soils would be drained whereas the less permeable soils would be undrained. In such cases it is logical and permissible in the same analysis to treat the drained soils in terms of effective stresses and the undrained soils in terms of total stresses.

4.1 Shear Strengths

Shear strengths for use in drained effective stress analyses can be measured in two ways:

1. In laboratory or field tests in which loads are applied slowly enough so that the soil is drained (there are no excess pore pressures) at failure, or
2. In laboratory tests such as consolidated-undrained (C-U) laboratory triaxial tests in which pore pressures are measured and the effective stresses at failure can be determined.

Effective stress strength envelopes determined using these two methods have been found to be, for all practical purposes, the same (Bishop and Bjerrum 1960).

Studies by Skempton and his colleagues (Skempton 1970, 1977, 1985) showed that peak drained strengths of stiff, overconsolidated clays determined in laboratory tests are larger than the drained strengths that can be mobilized in the field over a long period of time. Skempton recommended the use of "fully softened" strengths for stiff clays in which there has been no previous sliding. The fully softened strength is measured by remolding the clay in the laboratory at a water content near the liquid limit, reconsolidating it in the laboratory, and measuring its strength in a normally consolidated condition.

Once sliding has occurred in a clay, the clay particles become reoriented parallel to the slip surface, and the strength decreases progressively as sliding displacement occurs, eventually reaching a low residual value. Residual shear strengths should be used to analyze clay slopes in which slope failure by sliding has already occurred (Skempton 1970, 1977, 1985).

Morgenstern (1992) and others have pointed out that drained shear may cause structural collapse in certain sensitive or structured soils, resulting in development of excess pore pressures at a rate that is so rapid that drainage cannot occur. As a result, it is not possible to mobilize the full effective stress shearing resistance under drained conditions. These difficult soils (loose sands and sensitive and highly structured clays) deserve special attention (see Chapter 24 for sensitive clays).

For soils that are partly saturated, such as compacted clays or naturally occurring clayey soils from above the water table, undrained strengths should be measured using unconsolidated-undrained tests on specimens with the same void ratio and the same degree of saturation as the soil in the field. The undrained strength envelope for such soils is curved, and as a result the values of total stress c and ϕ from such tests are not unique. It is important therefore to use a range of confining pressures in the laboratory tests that corresponds to the range of pressures to which the soil is subjected in the field and to select values of c and ϕ that provide a reasonable representation of the strength of the soil in this pressure range. Alternatively, with some slope stability computer programs, it is possible to use a nonlinear strength envelope, represented by a series of points, without reference to c and ϕ.

For soils that are completely saturated, the undrained friction angle is zero ($\phi_u = 0$). Undrained strengths for saturated soils can be determined from unconsolidated-undrained tests or from C-U tests by the Stress History and Normalized Soil Engineering Properties (SHANSEP) procedure (Ladd and Foott 1974).

Unconsolidated-undrained tests are performed on undisturbed test specimens from the field. These tests define the undrained strength of the soil in the field at the time and location where the samples were obtained, provided that the samples are undisturbed. Although some procedures provide samples that are called "undisturbed," no sample is completely free of disturbance effects. For saturated clays, these effects usually cause the undrained strengths measured in laboratory tests to be smaller

than the undrained strength in the field. As a result, unconsolidated-undrained triaxial tests usually give conservative values of undrained strengths.

Ladd and Foott (1974) and others have shown that the effects of disturbance on undrained strength can be compensated for by consolidating clay specimens to higher pressures in the laboratory. Because consolidation to higher pressures produces higher undrained shear strengths, the strengths measured using C-U tests are not directly applicable to field conditions. Ladd and Foott described procedures for determining values of S_u/p (the ratio of undrained strength divided by consolidation pressure) from such tests. The undrained strength in the field is estimated by multiplying the value of S_u/p by the field consolidation pressure. The same procedure can be used to estimate current undrained strengths (using current consolidation pressures) or future undrained strengths (using consolidation pressures estimated for some future condition by means of consolidation analysis).

C-U tests should not be used to determine values of c and ϕ from "total stress" Mohr-Coulomb strength envelopes for use in total stress analyses. This procedure is not valid because the normal stresses used to plot the Mohr's circles of stress at failure are not valid total stresses. These stress circles are plotted using the effective stress at the time of consolidation plus the deviator stress at failure. This procedure is not consistent. The method described by Ladd and Foott avoids the inconsistencies of this method by relating undrained strengths measured in C-U tests to consolidation pressure without the use of c- and ϕ-values. The values of undrained strength (S_u), determined as recommended by Ladd and Foott, are combined with $\phi_u = 0$, the correct undrained friction angle for saturated materials.

4.2 Unit Weights and Water Pressures

The primary requirement in slope stability analyses is to satisfy equilibrium *in terms of total stresses*. This is true whether the analysis is an effective stress analysis (in which shear strengths are related to effective stresses) or a total stress analysis (in which shear strengths are related to total stresses). In either case total stress is the prime variable in terms of the fundamental mechanics of the problem because a correct evaluation of equilibrium conditions must include both earth and water forces.

For analyses in terms of effective stress, pore pressures are subtracted from total stresses on the base of each slice to determine the values of effective stress, to which the soil strengths are related. For total stress analyses, it is not necessary to subtract pore pressures because the strengths are related to the total stresses.

Slope stability problems can be correctly formulated so that equilibrium is satisfied in terms of total stresses by using total unit weights and external boundary water pressures. Total unit weights are moist unit weights above the water table and saturated unit weights below the water table. When water pressures act on submerged external slope boundaries, these pressures are a component of total stress, and they must be included for correct evaluation of equilibrium in terms of total stresses.

For hydrostatic (no-flow) water conditions, it is possible to perform effective stress analyses by using buoyant unit weights below the water table and ignoring external boundary water pressures and internal pore pressures. Effective stress analyses of nonhydrostatic conditions can be performed in a similar way if seepage forces are also included. These procedures are not as straightforward as using total unit weights and boundary water pressures, however. They involve essentially the same amount of effort in calculation for hydrostatic conditions and much more calculation when seepage forces have to be evaluated. Thus, these procedures are not useful except for one purpose. Using buoyant unit weights and excluding external boundary water pressures and pore pressures for a hydrostatic condition afford a means of checking some of the functions of a computer program.

5. SLOPE STABILITY CHARTS

The accuracy of charts for slope stability analyses is usually at least as good as the accuracy with which shear strengths can be evaluated. Chart analyses can be accomplished in a few minutes, even when shear strengths and unit weights are carefully averaged to achieve the best possible accuracy. Charts thus provide a rapid and potentially very useful means for slope stability analyses. They can be used to good advantage to perform preliminary analyses, to check detailed analyses, and often to make complete analyses.

5.1 Averaging Slope Profile, Shear Strengths, and Unit Weights

For simplicity, charts are developed for simple homogeneous slopes. To apply them to real conditions, it is necessary to approximate the real slope with an equivalent simple and homogeneous slope.

The most effective method of developing a simple slope profile for chart analysis is to begin with a cross section of the slope drawn to scale. On this cross section, using judgment, the engineer draws a geometrically simple slope that approximates the real slope as closely as possible.

To average the shear strengths for chart analysis, it is useful to know, at least approximately, the location of the critical slip surface. The charts contained in the following sections of this chapter provide a means of estimating the position of the critical circle. Average strength values are calculated by drawing the critical circle, determined from the charts, on the slope. Then the central angle of arc subtended within each layer or zone of soil is measured with a protractor. The central angles are used as weighting factors to calculate weighted average strength parameters, c_{avg} and ϕ_{avg}:

$$c_{avg} = \frac{\Sigma \delta_i c_i}{\Sigma \delta_i} \tag{13.4}$$

$$\phi_{avg} = \frac{\Sigma \delta_i \phi_i}{\Sigma \delta_i} \tag{13.5}$$

where

c_{avg} = average cohesion (stress units);
ϕ_{avg} = average angle of internal friction (degrees);
δ_i = central angle of arc, measured around the center of the estimated critical circle, within zone i (degrees);
c_i = cohesion in zone i (stress units); and
ϕ_i = angle of internal friction in zone i.

The one condition in which it is preferable not to use these straightforward averaging procedures is the case in which an embankment overlies a weak foundation of saturated clay, with $\phi = 0$. Straightforward averaging in such a case would lead to a small value of ϕ_{avg} (perhaps 2 to 5 degrees), and with $\phi_{avg} > 0$, it would be necessary to use a chart like the one in Figure 13-6, which is based entirely on circles that pass through the toe of the slope, often not critical for embankments on weak saturated clays. With $\phi = 0$ foundation soils, the critical circle usually goes as deep as possible in the foundation, passing below the toe of the slope. In these cases it is better to approximate the embankment as a $\phi = 0$ soil and to use a $\phi = 0$ chart of the type shown in Figure 13-3. The equivalent $\phi = 0$ strength of the embankment soil can be estimated by calculating the average normal stress on the part of the slip surface within the embankment (one-half the average vertical stress is usually a reasonable approximation) and determining the corresponding shear strength at that point on the shear strength envelope for the embankment soil. This value of strength is treated as a value of S_u for the embankment, with $\phi = 0$. The average value of S_u is then calculated for both the embankment and the foundation using the same averaging procedure as described above:

$$(S_u)_{avg} = \frac{\Sigma \delta_i (S_u)_i}{\Sigma \delta_i} \tag{13.6}$$

where $(S_u)_{avg}$ is the average undrained shear strength (in stress units), $(S_u)_i$ is S_u in layer i (in stress units), and δ_i is as defined previously. This average value of S_u is then used, with $\phi = 0$, for analysis of the slope.

To average unit weights for use in chart analysis, it is usually sufficient to use layer thickness as a weighting factor, as indicated by the following expression:

$$\gamma_{avg} = \frac{\Sigma \gamma_i h_i}{\Sigma h_i} \tag{13.7}$$

where

γ_{avg} = average unit weight (force per length cubed),
γ_i = unit weight of layer i (force per length cubed), and
h_i = thickness of layer i (in length units).

Unit weights should be averaged only to the depth of the bottom of the critical circle.

If the material below the toe of the slope is a $\phi = 0$ material, the unit weight should be averaged only down to the toe of the slope, since the unit weight of the material below the toe has no effect on stability in this case.

5.2 Soils with $\phi = 0$

Stability charts for slopes in $\phi = 0$ soils are shown in Figure 13-3. These charts, as well as the related

ones in Figures 13-4, 13-5, and 13-6, were developed by Janbu (1968).

The coordinates of the center of the critical circle are given by

$$X_0 = x_0 H \quad (13.8)$$

$$Y_0 = y_0 H \quad (13.9)$$

where

X_0, Y_0 = coordinates of critical circle center measured from toe of slope,

x_0, y_0 = dimensionless numbers determined from charts at bottom of Figure 13-3, and

H = height of slope.

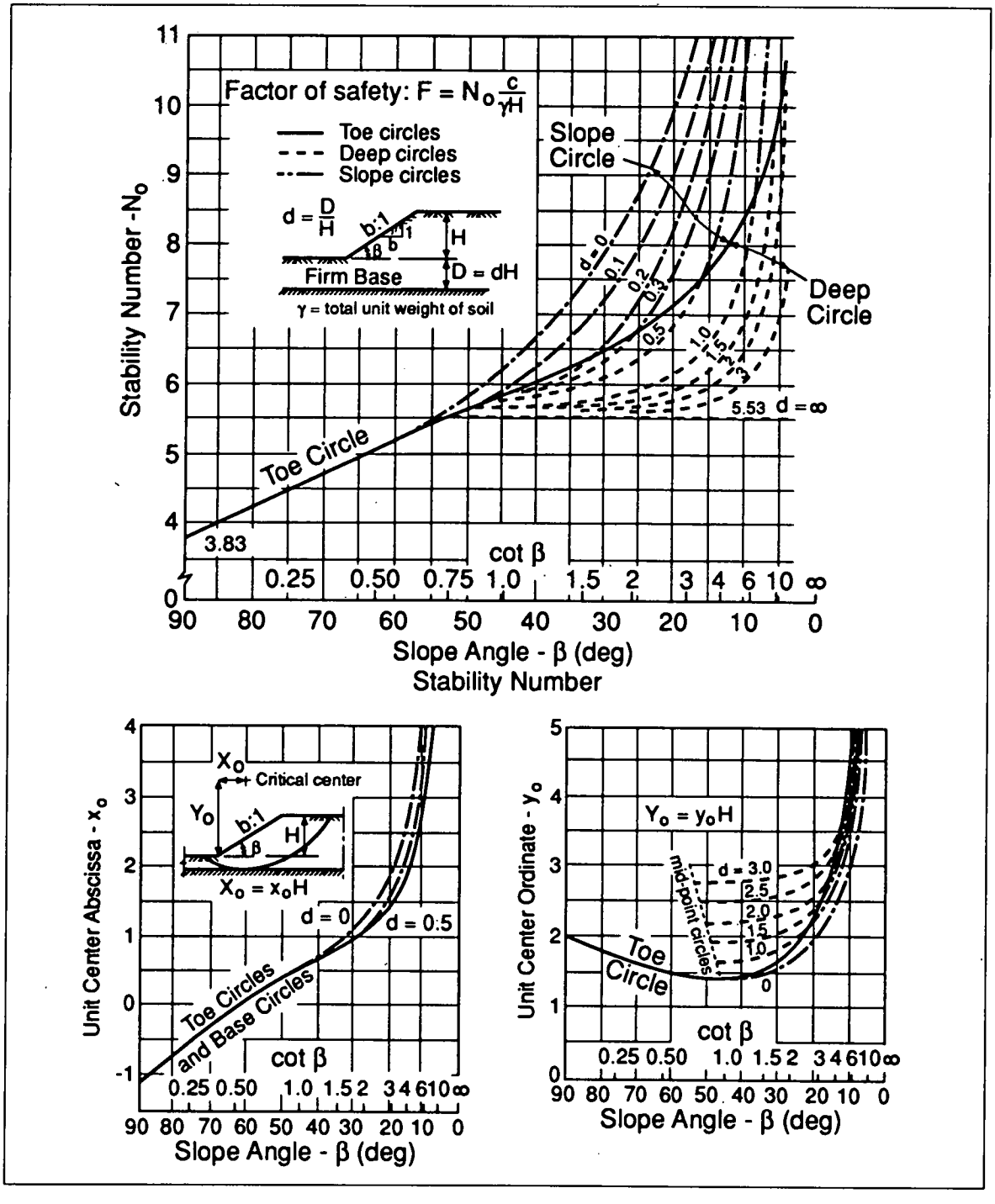

FIGURE 13-3
Slope stability charts for $\phi = 0$ soils (modified from Janbu 1968).

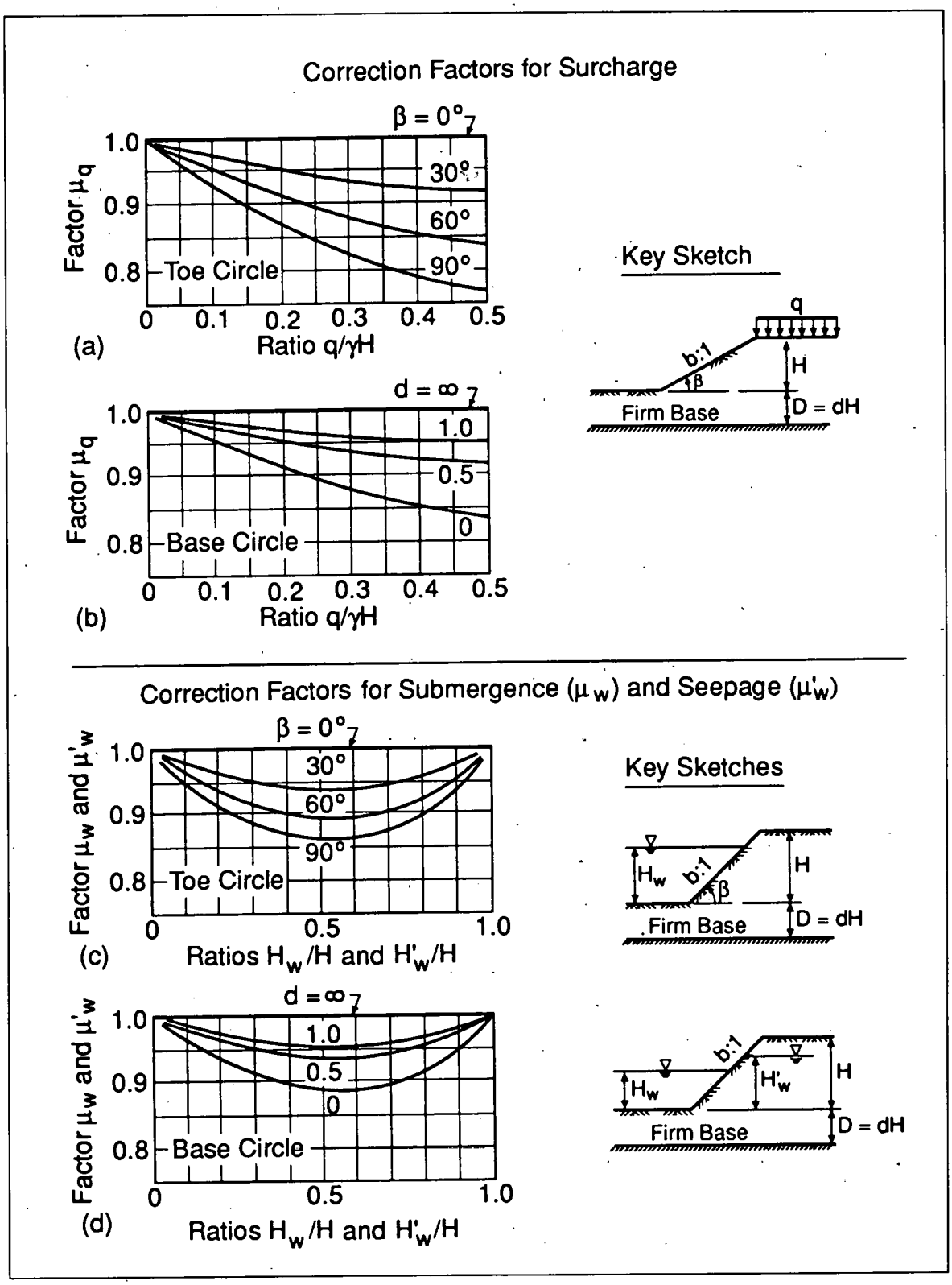

FIGURE 13-4 Correction factors for slope stability charts for $\phi = 0$ and $\phi > 0$ soils for cases with surcharge, submergence, or seepage (modified from Janbu 1968).

FIGURE 13-5
Correction factors for slope stability charts for $\phi = 0$ and $\phi > 0$ soils for cases with tension cracks (modified from Janbu 1968).

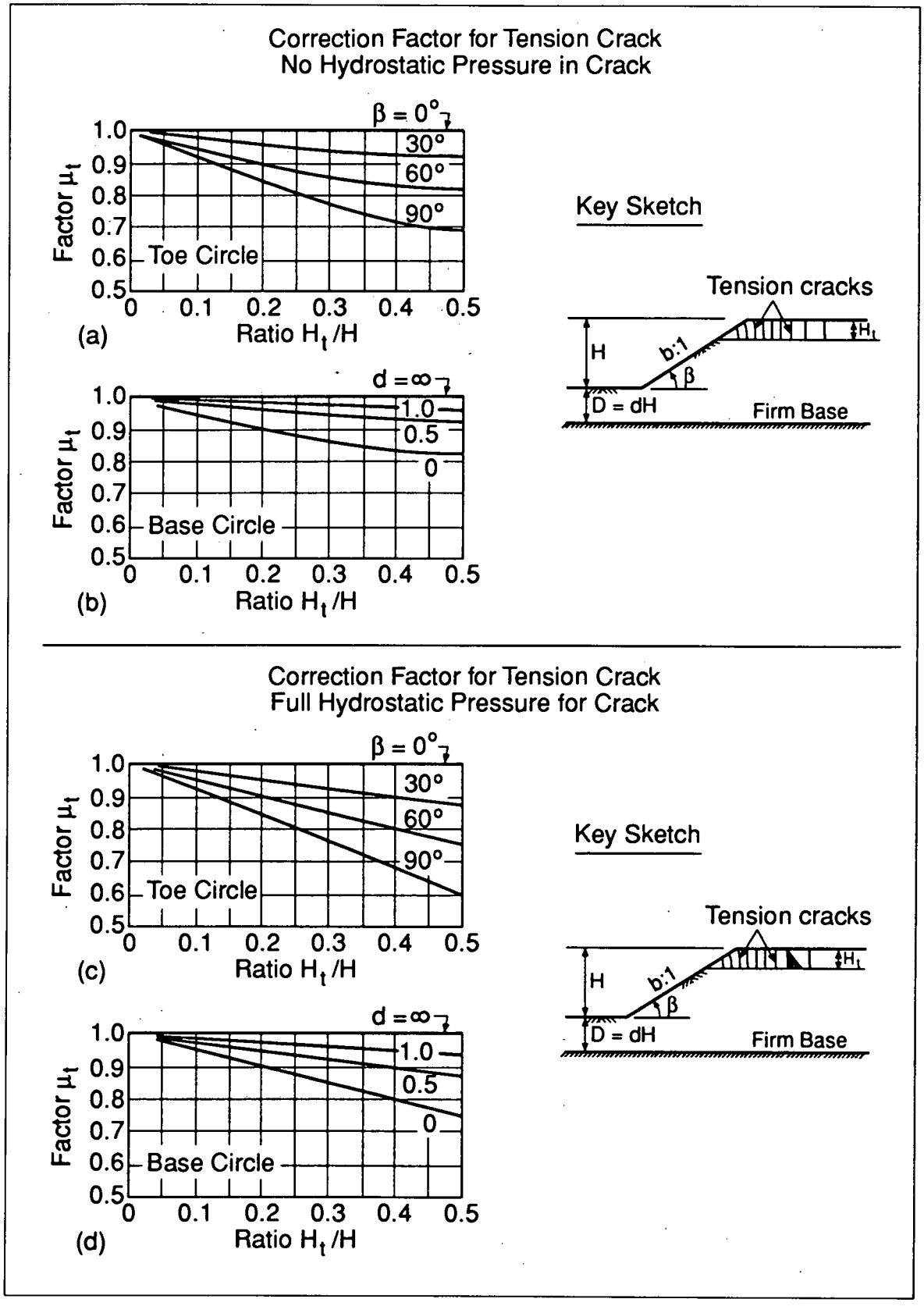

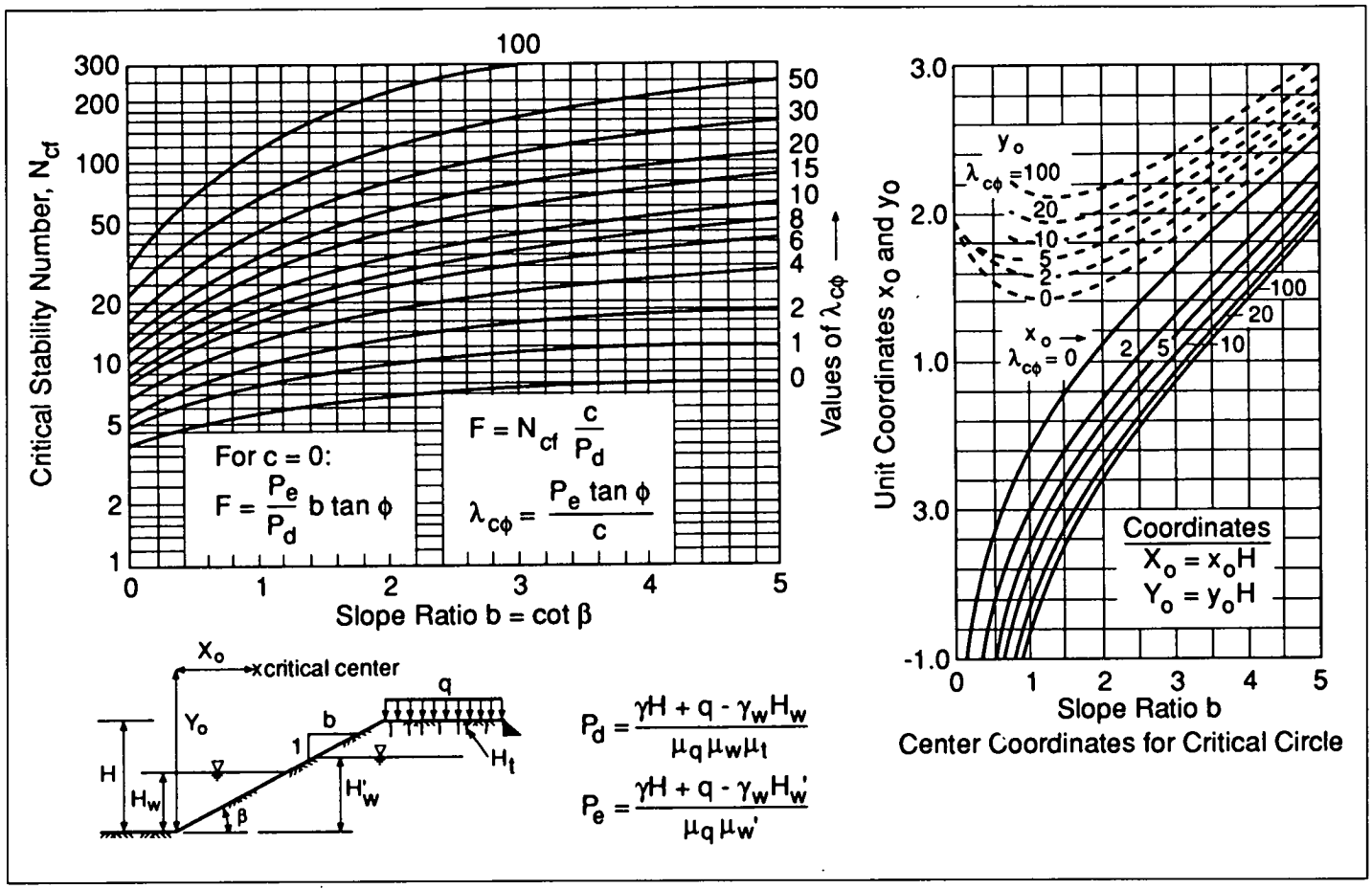

FIGURE 13-6
Slope stability charts for $\phi > 0$ soils (modified from Janbu 1968).

The radius of the critical circle is determined by the position of the center of the circle and the fact that the circle is tangent to a horizontal plane at depth D below the bottom of the slope. Using the chart in Figure 13-3, it is possible to calculate factors of safety for a range of depths (D) to determine which is most critical. If the value of S_u in the foundation does not vary with depth, the critical circle will extend as deep as possible, and only a circle extending through the full depth of the clay layer need be analyzed. If the strength of the foundation clay increases with depth, the critical circle may or may not extend to the base of the layer, and it is necessary to examine various depths to determine which is most critical.

The upper part of Figure 13-3 gives values of the stability number, N_0, which is related to the factor of safety by the expression

$$F = N_0 \frac{c}{P_d} \tag{13.10}$$

where

F = factor of safety (dimensionless),
N_0 = stability number from Figure 13-3 (dimensionless), and
$c = S_u$ = undrained shear strength (in stress units).

The value of P_d is given by the expression

$$P_d = \frac{\gamma H + q - \gamma_w H_w}{\mu_q \mu_w \mu_t} \tag{13.11}$$

where

P_d = driving force term (in pressure units),
γ = unit weight (force per length cubed),
H = slope height (length),
q = surcharge pressure on top of slope (in stress units),
γ_w = unit weight of water (force per length cubed),
H_w = depth of water outside slope, measured above toe (length),
μ_q = surcharge correction factor,
μ_w = water pressure correction factor, and
μ_t = tension crack correction factor.

The correction factors μ_q, μ_w, μ_t are given in Figures 13-4 and 13-5.

5.3 Soils with $\phi > 0$

In most cases for slopes in soils with $\phi > 0$, the critical slip circle passes through the toe of the slope. The stability chart shown in Figure 13-6 is based on the assumption that this is true. The coordinates of the center of the critical toe circle are shown in the chart on the right side of Figure 13-6.

Cohesion values, friction angles, and unit weights are averaged using the procedures described at the beginning of this chapter. The factor of safety is calculated using the expression

$$F = N_{cf} \frac{c}{P_d} \tag{13.12}$$

where N_{cf} is the stability coefficient from the chart on the left-hand side of Figure 13-6 (dimensionless), c is the average cohesion intercept (in stress units), and P_d is defined by Equation 13.11.

The values of N_{cf} shown in Figure 13-6 are determined by the value of b = cotangent of the slope angle = cot ß and the value of the dimensionless parameter, $\lambda_{c\phi}$. The latter is calculated using the expression

$$\lambda_{c\phi} = \frac{P_e \tan\phi}{c} \tag{13.13}$$

where c and $\tan\phi$ are the average values of cohesion intercept and friction angle. The value of P_e is defined as

$$P_e = \frac{\gamma H + q - \gamma_w H_w'}{\mu_q \mu_w'} \tag{13.14}$$

where H_w' is the effective average water level inside the slope measured above the toe of the slope (in length units), μ_w' is the seepage correction factor from the lower part of Figure 13-4, and γ, H, q, and μ_q are as defined previously.

The value of H_w', somewhat difficult to estimate using judgment, is related to H_c, the water level measured below the crest of the slope, as shown in Figure 13-7. When the value of H_c has been determined by field measurements or seepage analyses, the value of H_w' can be determined using the curve given in Figure 13-7.

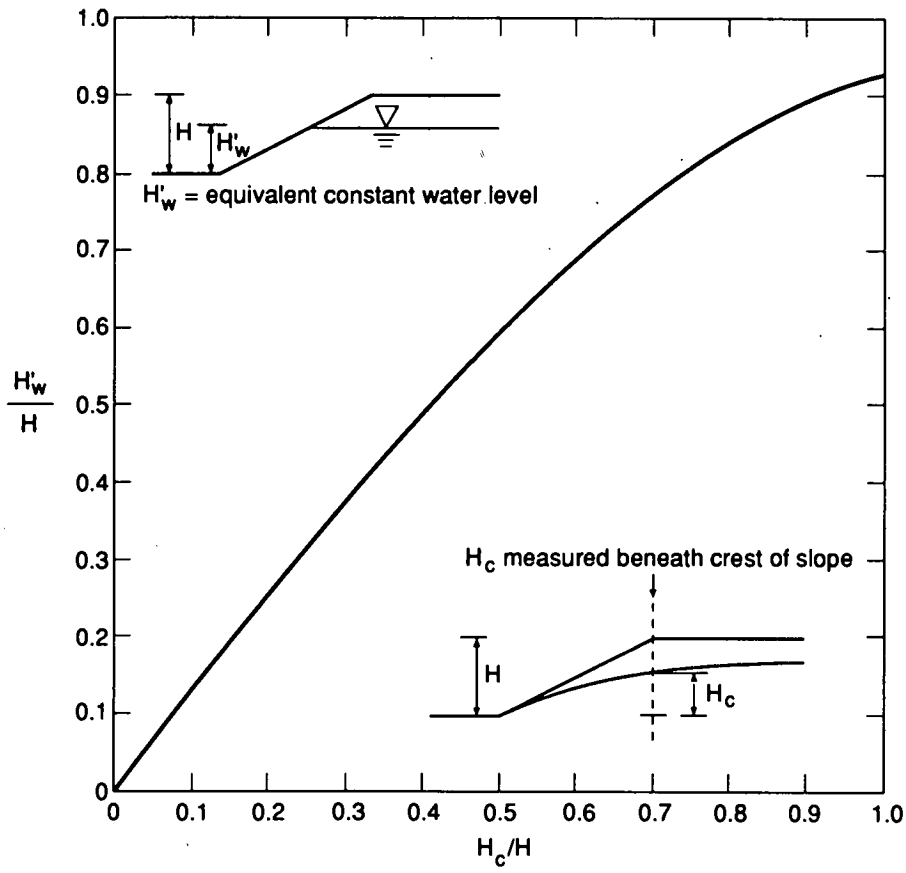

FIGURE 13-7 Chart for determining steady seepage conditions (modified from Duncan et al. 1987).

5.4 Infinite Slope Analyses

Conditions are sometimes encountered in which a layer of firm soil or rock lies parallel to the surface of the slope at shallow depth. In such conditions the slip surface is constrained to parallel the slope, as shown in Figure 13-8. When such slip surfaces are long compared with their depth, they can be approximated accurately by infinite slope analyses. Such analyses ignore the driving force at the upper end of the slide mass and the resisting force at the lower end. The resisting force is ordinarily greater, and infinite slope analyses are therefore somewhat conservative.

The factor of safety for infinite slope analyses can be expressed as

$$F = A\,\frac{\tan\phi'}{\tan\beta} + B\,\frac{c'}{\gamma H} \qquad (13.15)$$

where

A, B = dimensionless stability coefficients given in Figure 13-8,
ϕ', c' = effective stress strength parameters for slip surface,
β = slope angle,
γ = unit weight of sliding mass (force per length cubed), and

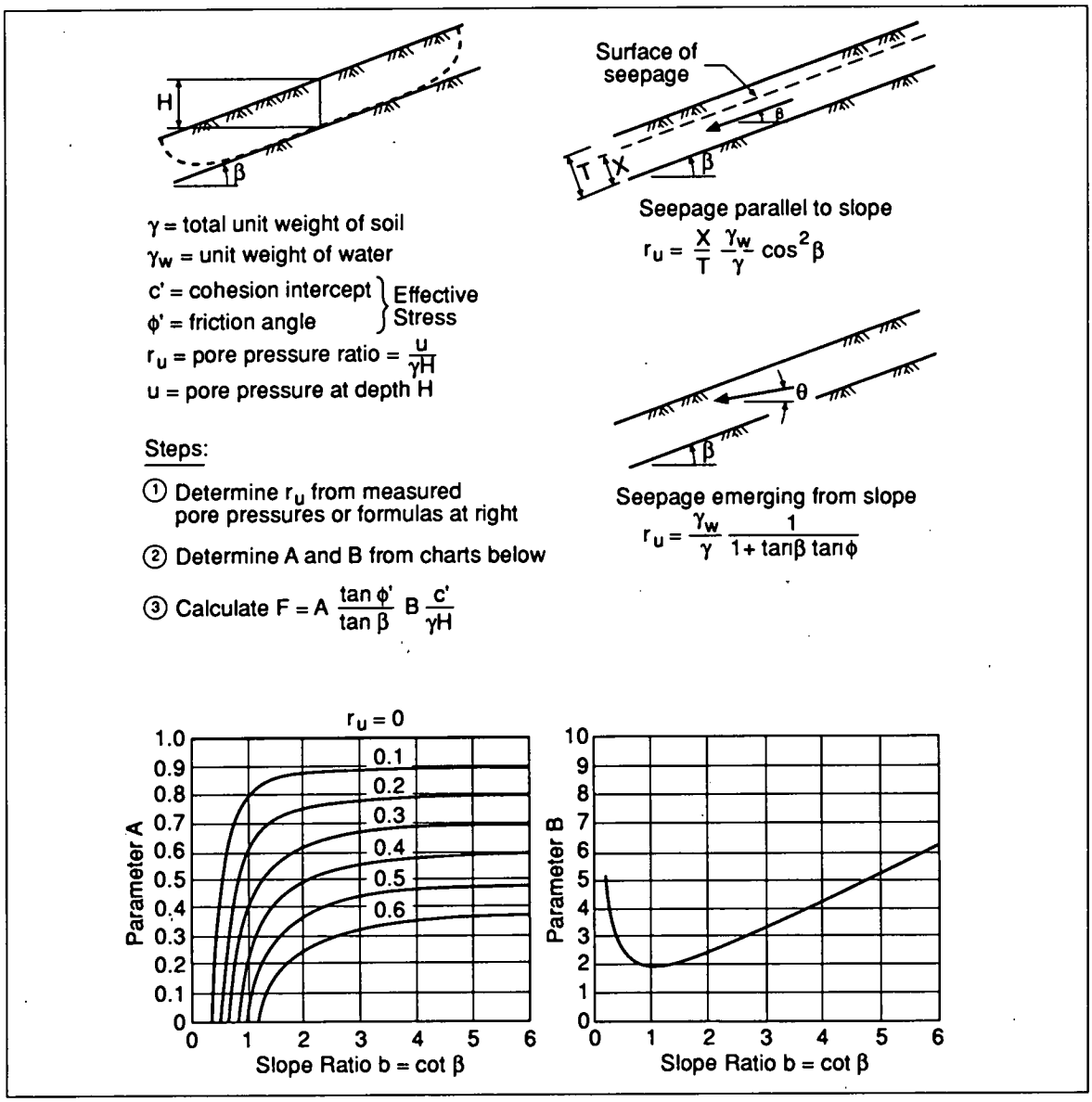

FIGURE 13-8 Stability charts for infinite slopes (modified from Duncan et al. 1987).

H = depth measured vertically from slope surface to slip surface (in length units).

The charts shown in Figure 13-8 can be used for effective stress or total stress analyses. For effective stress analyses, the pore pressures along the slip surface are characterized by the dimensionless pore-pressure ratio, r_u, as indicated in Figure 13-8. For total stress analyses, c and ϕ (total stress shear strength parameters) are used instead of c' and ϕ', and the value of r_u is equal to zero.

5.5 Soils with ϕ = 0 and Strength Increasing with Depth

The undrained shear strengths of normally consolidated clays usually increase with depth. The strength profile for this condition can often be approximated by a straight line, as shown in Figure 13-9. The factor of safety for slopes in such deposits can be expressed as

$$F = N \frac{c_b}{\gamma (H + H_0)} \tag{13.16}$$

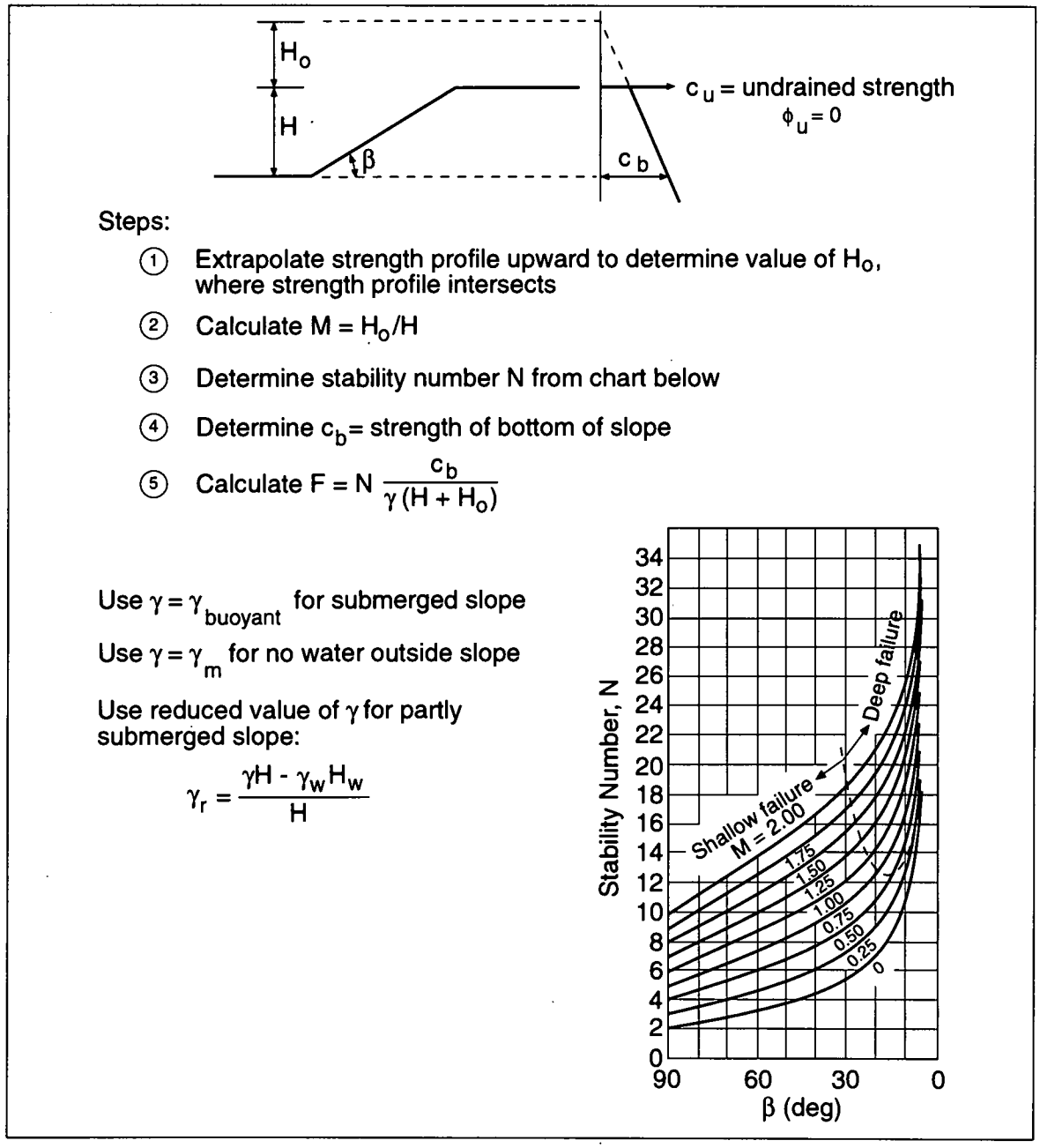

FIGURE 13-9
Slope stability charts for ϕ = 0 and strength increasing with depth (modified from Hunter and Schuster 1968).

where

N = dimensionless stability coefficient from Figure 13-9,
c_b = undrained shear strength (S_u) at elevation of toe of slope (in stress units),
γ = unit weight of soil (force per length cubed),
H = slope height (length), and
H_0 = height above top of slope where strength profile, projected upward, intersects zero strength (in length units).

Figure 13-9 can be used to analyze subaerial slopes or slopes that are submerged in water. For subaerial slopes the total (moist or saturated) unit weight is used. For submerged slopes the buoyant unit weight ($\gamma_b = \gamma_{sat} - \gamma_w$) is used. A reduced value of γ, calculated using the following expression, can be used for partly submerged slopes:

$$\gamma_r = \frac{\gamma H - \gamma_w H_w}{H} \tag{13.17}$$

where γ_r is the value of unit weight reduced for partial submergence, and the other terms are as defined previously.

6. DETAILED ANALYSES

Detailed analyses of slope stability are needed whenever it is necessary to include details of slope configuration, soil property zonation, or shape of the slip surface that cannot be represented in chart analyses. If a computer and slope stability computer program are available, detailed analyses can be performed efficiently, including a thorough search for the critical slip surface. If a computer is not available, detailed analyses can be performed manually using the procedures described in the following section. Even when analyses are performed using a computer, it is good practice to check the factor of safety for the critical slip surface using manual calculations. The U.S. Army Corps of Engineers (1970) requires such calculations for the critical slip surface for all important slope stability analyses.

6.1 Manual Calculations

It is convenient to use a tabular computation form to perform manual calculations of slope stability. Calculations that are well organized are easy to check. In the following sections, tabular computation forms are given for the ordinary method of slices, Bishop's modified method, and a force equilibrium method with the same side force inclination on all slices.

6.1.1 Ordinary Method of Slices

A tabular form for the ordinary method of slices is presented in Figure 13-10, and example calculations made using this form are given in Figure 13-11. The slope to which the calculations apply is shown in Figure 13-12.

The slice weights in the second column were calculated on the basis of the dimensions of the slices and the unit weights of the soils within them. A simple method of calculating slice weights, shown in Figure 13-12, uses

$$W = b\Sigma(\gamma_i h_i) \tag{13.18}$$

where

W = slice weight (force per unit length),
b = width of slice (length),
γ_i = unit weight of soil i (force per length cubed), and
h_i = height of soil layer i where it is subtended by slice (length).

Values of h_i are measured at the center of the slice. Equation 13.18 can be applied to triangular as well as quadrilateral slices.

The base length l and the base angle α for each slice are measured on a scale drawing of the slope and slip surface. The values of c and ϕ for each slice correspond to the type of soil at the bottom of the slice, and slices are drawn so that the base of each slice is in only one type of soil. The value of u for each slice is the average value at the middle of the base. Slices need not be of equal width.

The quantities in the last two columns (N_1 and N_2) can be calculated using the tabulated values for each slice. These two columns are summed, and the factor of safety is calculated as shown in the bottom right corner of the computation form (Figure 13-11). For the example shown, the ordinary method of slices factor of safety is 1.43.

6.1.2 Bishop's Modified Method

A tabular computation form for Bishop's modified method is shown in Figure 13-13, and calculations

Slice No.	W	l	α	c	ϕ	u	N_1	N_2
1								
2								
3								
4								
5								
6								
7								
8								
9								
10								
11								
12								
13								
14								
15								
						$\Sigma =$		

W = weight of slice - kN/m

c = cohesion intercept - kN/m^2

ϕ = friction angle - degrees

u = pore pressure - kN/m^2

α = angle between base of slice and horizontal - degrees

l = length of slip surface segments measured along base of slice - m

$N_1 = W \sin \alpha$

$N_2 = [W \cos \alpha - ul] \tan \phi + cl$

$F = \Sigma (N_2) / \Sigma (N_1) =$ ____

FIGURE 13-10 Tabular computation form for ordinary method of slices.

for the example slope shown in Figure 13-12 are given in Figure 13-14. The first eight columns in the form are the same as those for the ordinary method of slices.

The value of the quantity N_2 for Bishop's modified method depends on the factor of safety, as shown by the expression for N_2 at the bottom of the form.

Because N_2 depends on the factor of safety and the factor of safety also depends on N_2, it is necessary to use repeated trials to calculate the factor of safety by Bishop's modified method. For this reason, four columns are shown for N_2, each corresponding to a different value of the assumed factor of safety, F_a. The first value assumed for F_a was 1.43, the value calculated using the ordinary method of slices; this value is shown at the top of the ninth column (Figure 13-14). Using the resulting values of N_2 (the values in the ninth column), the value of F_c (the calculated factor of safety) was found to equal 1.51. When this value was used as F_a, F_c was 1.52. When 1.52 was used as the value of F_a, F_c was also 1.52, indicating that the assumed value was correct and no further iteration was needed.

It can be seen that the value of F calculated using Bishop's modified method (1.52) is larger than the value calculated using the ordinary method of slices (1.43), as is usually the case. For effective stress analyses with high pore pressures, the difference may be much larger than the 6 percent difference in this case, indicating significant inaccuracy in the ordinary method of slices for effective stress analyses with high pore pressures.

Slice No.	W	l	α	c	ϕ	u	N_1	N_2
1	112	5.3	-32.0	35.9	0.0	0	-60	191
2	297	4.9	-22.0	35.9	0.0	0	-111	177
3	499	4.7	-13.0	35.9	0.0	0	-112	169
4	726	4.6	-4.0	35.9	0.0	0	-51	165
5	903	4.6	4.0	35.9	0.0	0	63	165
6	1,028	4.7	13.0	35.9	0.0	0	231	169
7	1,003	4.9	22.0	35.9	0.0	0	376	177
8	818	5.3	32.0	35.9	0.0	0	433	191
9	587	6.7	43.0	4.8	35.0	0	400	333
10	128	5.6	55.0	4.8	35.0	0	105	79
11							0	0
12							0	0
13							0	0
14							0	0
15							0	0
						$\Sigma =$	1274	1816

W = weight of slice - kN/m

c = cohesion intercept - kN/m^2

ϕ = friction angle - degrees

u = pore pressure - kN/m^2

α = angle between base of slice and horizontal - degrees

l = length of slip surface segments measured along base of slice - m

$N_1 = W \sin \alpha$

$N_2 = [W \cos \alpha - ul] \tan \phi + cl$

$F = \Sigma (N_2) / \Sigma (N_1) = \underline{1.43}$

FIGURE 13-11 Example computation for ordinary method of slices.

Numerical problems sometimes arise with Bishop's modified method. These difficulties arise at the top or bottom ends of the slip circle, where the bases of the slices are steep. When these numerical problems arise, the value of the factor of safety calculated by Bishop's modified method may be smaller than the value calculated by the ordinary method of slices, rather than larger. When this happens, it is reasonable to use the *F*-value determined by the ordinary method of slices rather than that determined by Bishop's modified method. To check for these numerical problems, it is useful to calculate *F* by the ordinary method of slices to determine whether it is smaller or larger than the value from Bishop's modified method.

6.1.3 Force Equilibrium with Constant Side Force Inclination

The ordinary method of slices and Bishop's modified method can only be used to analyze circular slip surfaces. It is useful to have a method that can be used for manual calculations of noncircular slip surfaces in order to check computer analyses or to perform analyses when a computer is not available. A tabular form for force equilibrium analyses with the same side force inclination on every slice is shown in Figure 13-15, and an example of the use of this form is shown in Figure 13-16. Figure 13-17 shows the slope analyzed in Figure 13-16, a sand embankment on a clay foundation.

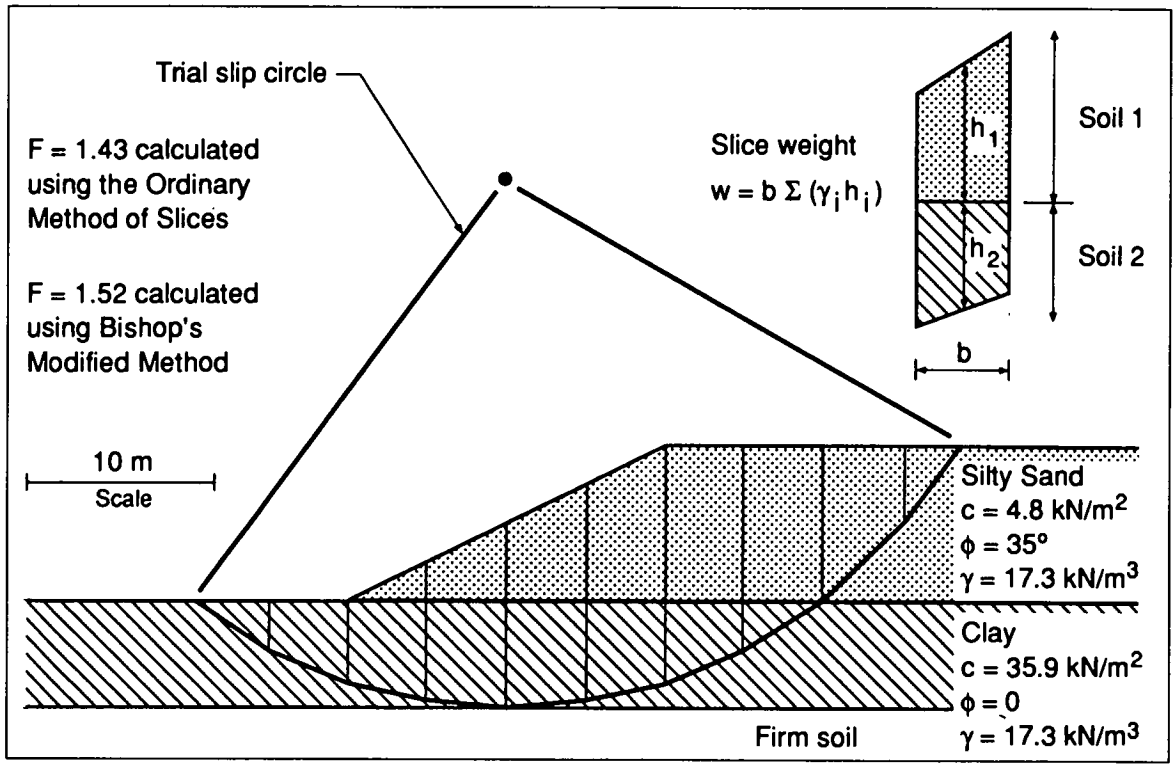

FIGURE 13-12 Example slope: sand embankment over clay foundation.

The seven columns in the upper section of the form contain the same information regarding the slices as shown in the first seven columns of the form for the ordinary method of slices and Bishop's modified method. Note that the assumed value of θ is listed at the top of the upper section of the form. Values of θ must be assumed for all force equilibrium methods.

The calculations for ΔE, the unbalanced force on each slice, involve the five quantities N_0, N_1, N_2, N_3, and N_4. Expressions for these terms are given in the lower part of the form. The values of all of these terms depend on the value of the factor of safety, and iteration is therefore needed to evaluate F. This involves assuming a value for F and checking to see if the forces balance. The forces balance when $\Sigma\Delta E = 0$.

The middle section of the form is labeled Trial 1 and the lower section is labeled Trial 2. Each trial corresponds to a new value of F_a (the assumed value of the factor of safety). The solution is achieved by assuming a value of F_a and using the tabular form to calculate $\Sigma\Delta E$. If $\Sigma\Delta E$ is positive, the assumed factor of safety is too high, and a lower value is assumed for the next trial. If $\Sigma\Delta E$ is negative, a larger value of F_a is assumed for the next trial. The assumed value of F is the correct value when $\Sigma\Delta E = 0$. If more than two trials are needed to find the correct value of F, as is commonly the case, additional copies of the form are used for those calculations.

For the example shown in Figure 13-17, the factor of safety is 2.44 for θ = 10 degrees. This is shown by the calculations in Figure 13-16. Other calculations, not shown, resulted in values of F = 1.96 for θ = 0, and F = 3.38 for θ = 20 degrees. The variation of F with θ for this example is shown in Figure 13-18.

It is clear from the results shown in Figure 13-18 that the factor of safety from force equilibrium solutions varies significantly with the assumed value of θ. In this particular example, the computed factor of safety increases by 72 percent (from 1.96 to 3.38) as the side force angle θ is varied from zero to 20 degrees. This illustrates the importance of having a reasonable estimate of the value of θ when the force equilibrium method is used.

The best way to determine the value of θ is by use of the condition of moment equilibrium. Spencer's method, like the method of analysis on which the computation form in Figure 13-15 is based, assumes a constant value of θ. However,

							F_a =				
Slice No.	W	l	α	c	ϕ	u	N_1	N_2	N_2	N_2	N_2
1											
2											
3											
4											
5											
6											
7											
8											
9											
10											
11											
12											
13											
14											
15											
							Σ=				
							F_c=				

W = weight of slice - kN/m
ϕ = friction angle - degrees
c = cohesion intercept - kN/m^2
u = pore pressure - kN/m^2

α = angle between base of slice and horizontal - degrees

l = length of slip surface segments measured along base of slice - m
F_a = assumed F
F_c = calculated F

$$N_1 = W \sin \alpha$$

$$N_2 = \frac{\left\{\left[\frac{W}{\cos \alpha} - ul\right] \tan \phi + cl\right\}}{\left[1 + \frac{\tan \alpha \tan \phi}{F_a}\right]}$$

$$F_c = \Sigma (N_2) / \Sigma (N_1) = \_\_\_\_$$

FIGURE 13-13 Tabular computation form for Bishop's modified method.

Spencer's method satisfies moment equilibrium as well as force equilibrium. Only one value of θ satisfies both force and moment equilibrium. For the example shown in Figure 13-17, the value that satisfies moment equilibrium is θ = 13.5 degrees, and the corresponding factor of safety is F = 2.69. This value of F is the best estimate of the factor of safety for this slope and slip surface. It would differ by no more than about 12 percent from the value of F calculated using any other method that satisfied all conditions of equilibrium and that involved reasonable assumptions.

The trend of F with assumed value of θ shown in Figure 13-18 is typical. As the assumed value of θ for a force equilibrium solution increases, the calculated value of F also increases. It is almost always conservative to assume that θ = 0 degrees, and it is almost always unconservative to assume that θ equals the slope angle. Thus, although the method outlined by the form given in Figure 13-15 can be used to check Spencer's method calculations precisely, it has limited value as an independent method of calculating F because of the strong dependence of the calculated value of F on the assumed value of θ. The same is true of all force equilibrium methods.

6.2 Computer Analyses

As shown in the preceding sections, slope stability analyses involve lengthy calculations. Use of a computer for these calculations has great potential in two respects:

1. Computer analyses make it possible to perform calculations by advanced methods that satisfy all

							F_a =	1.43	1.51	1.52	
Slice No.	W	l	α	c	ϕ	u	N_1	N_2	N_2	N_2	N_2
1	112	5.3	-32.0	35.9	0.0	0	-60	192	192	192	
2	297	4.9	-22.0	35.9	0.0	0	-111	177	177	177	
3	499	4.7	-13.0	35.9	0.0	0	-112	170	170	170	
4	726	4.6	-4.0	35.9	0.0	0	-51	165	165	165	
5	903	4.6	4.0	35.9	0.0	0	63	165	165	165	
6	1,028	4.7	13.0	35.9	0.0	0	231	170	170	170	
7	1,003	4.9	22.0	35.9	0.0	0	376	177	177	177	
8	818	5.3	32.0	35.9	0.0	0	433	192	192	192	
9	587	6.7	43.0	4.8	35.0	0	400	408	415	416	
10	128	5.6	55.0	4.8	35.0	0	105	108	111	111	
11							0	0	0	0	
12							0	0	0	0	
13							0	0	0	0	
14							0	0	0	0	
15							0	0	0	0	
							Σ=	1,275	1,925	1,934	1,935
							Fc=	1.51	1.52	1.52	

W = weight of slice - kN/m
c = cohesion intercept - kN/m^2
ϕ = friction angle - degrees
u = pore pressure - kN/m^2
α = angle between base of slice and horizontal - degrees
l = length of slip surface segments measured along base of slice - m
F_a = assumed F
F_c = calculated F

$$N_1 = W \sin \alpha$$

$$N_2 = \frac{\left\{\left[\frac{W}{\cos \alpha} - ul\right] \tan \phi + cl\right\}}{\left[1 + \frac{\tan \alpha \tan \phi}{F_a}\right]}$$

$$F_c = \Sigma (N_2) / \Sigma (N_1) = \_\_\_\_$$

FIGURE 13-14 Example computation for Bishop's modified method.

conditions of equilibrium. This advantage reduces the uncertainty resulting from the method of calculation to ±6 percent. Note that this is only the uncertainty due to the method of analysis. The overall uncertainty, including the uncertainty involved in the estimated values of shear strength, is almost always considerably larger.

2. Computer analyses make it possible to conduct a thorough search for the critical circle or critical noncircular slip surface. Because the calculations for a single slip surface take 1 to 3 hr by hand, it is not feasible to search for these values as thoroughly as it is using computer analyses.

6.2.1 Computer and Computer Program Selection

Practically any personal computer can be used for slope stability analyses. A thorough search for the critical slip surface can be accomplished in 10 min or so using a 286-class personal computer and in 1 min or so using a 486-class personal computer.

The most important aspect of computer analysis is the computer program. Programs are being developed continuously to provide a wider range of capabilities and to offer greater ease of use. The optimum computer program for slope stability analysis should have these features:

- It should be based on an advanced method of analysis that satisfies all conditions of equilibrium. It should also be capable of performing calculations using other methods, such as the ordinary method of slices, Bishop's modified method, and force equilibrium methods if the user needs them.
- It should be efficient in terms of the time required for input and output. The cost of com-

θ =

Slice	Weight	l	α	c	ϕ	u
1						
2						
3						
4						
5						
6						

Trial #1 F_a =

Slice	N_0	N_1	N_2	N_3	N_4	ΔE
1						
2						
3						
4						
5						
6						

$\Sigma\Delta E$ =

Trial #2 F_a =

Slice	N_0	N_1	N_2	N_3	N_4	ΔE
1						
2						
3						
4						
5						
6						

$\Sigma\Delta E$ =

$$N_0 = \frac{\sin\alpha - \cos\alpha \tan\phi / F}{\cos\alpha + \sin\alpha \tan\phi / F}$$

$$N_1 = W N_0$$

$$N_2 = \frac{c\,l}{F}(\cos\alpha + N_0 \sin\alpha)$$

$$N_3 = u\,l\,(\sin\alpha - N_0 \cos\alpha)$$

$$N_4 = \cos\theta + N_0 \sin\theta$$

$$\Delta E = (N_1 - N_2 + N_3) / N_4$$

θ = side force angle - degrees

W = weight of slice - kN/m

ϕ = friction angle - degrees

α = slice base angle - degrees

F_a = assumed F

c = cohesion intercept - kN/m^2

u = pore pressure - kN/m^2

l = length of slice base - m

FIGURE 13-15 Tabular computation form for force equilibrium method with constant θ.

puter resources for slope stability analyses is usually very small when the cost of equipment and programs is spread over a large number of analyses. The cost of engineering time for input and output is far greater. Therefore it is important that the computer program be designed to minimize the personnel time required for analyses.

- It should be capable of analyzing all the conditions of interest to the user. These will always include undrained conditions, drained conditions, ponded water outside the slope, and internal

FIGURE 13-16
Example computation for force equilibrium.

Theta = 10

Slice	Weight	l	α	c	ϕ	u
1	50.5	3.52	60.00	0.0	30.00	0.00
2	77.1	1.73	45.00	24.0	0.00	0.00
3	189.2	3.66	0.00	24.0	0.00	0.00
4	21.0	1.73	-45.00	24.0	0.00	0.00
5						
6						

Trial #1 F_a = 2.30

Slice	N_0	N_1	N_2	N_3	N_4	ΔE
1	1.03	52.13	0.00	0.00	1.16	44.78
2	1.00	77.10	25.42	0.00	1.16	44.61
3	0.00	0.00	38.11	0.00	0.98	-38.70
4	-1.00	-21.00	25.42	0.00	0.81	-57.22
5						
6						

ΣΔE = -6.53

Trial #2 F_a = 2.44

Slice	N_0	N_1	N_2	N_3	N_4	ΔE
1	1.06	53.61	0.00	0.00	1.17	45.86
2	1.00	77.10	23.91	0.00	1.16	45.91
3	0.00	0.00	35.85	0.00	0.98	-36.41
4	-1.00	-21.00	23.91	0.00	0.81	-55.36
5						
6						

ΣΔE = 0.00

$$N_0 = \frac{\sin\alpha - \cos\alpha \tan\phi / F}{\cos\alpha + \sin\alpha \tan\phi / F}$$

$$N_1 = W N_0$$

$$N_2 = \frac{c\,l}{F}(\cos\alpha + N_0 \sin\alpha)$$

$$N_3 = u\,l\,(\sin\alpha - N_0 \cos\alpha)$$

$$N_4 = \cos\theta + N_0 \sin\theta$$

$$\Delta E = (N_1 - N_2 + N_3) / N_4$$

θ = side force angle - degrees

W = weight of slice - kN/m

ϕ = friction angle - degrees

α = slice base angle - degrees

F_a = assumed F

c = cohesion intercept - kN/m^2

u = pore pressure - kN/m^2

l = length of slice base - m

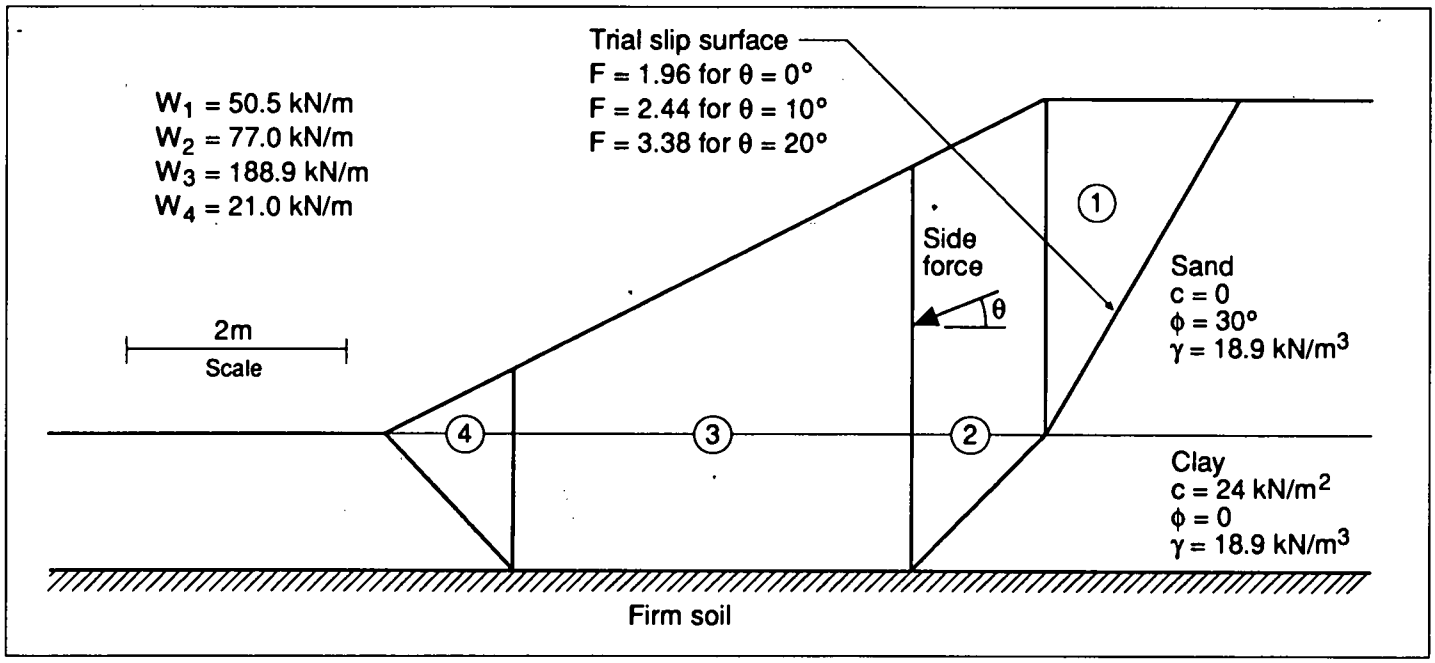

FIGURE 13-17
Noncircular slip surface, force equilibrium analysis.

pore-water pressures. Other conditions that may be of interest include rapid drawdown, slopes with reinforcement, pseudostatic seismic loading, and concentrated or distributed loads on slopes.

Selection of a suitable computer program is an important matter, worthy of careful research and evaluation. It is important to bear in mind that the initial outlay for the computer program is less important than its capabilities, its reliability, and its efficiency as measured in terms of personnel time required to perform analyses. Program distributors and users can provide the information required to make a selection. Because computer programs for slope stability are being improved constantly, acquiring a new program from time to time is a logical method of improving efficiency and effectiveness. Suitable programs may be identified by recommendations of professional colleagues or by review of professional papers and advertisements in technical publications.

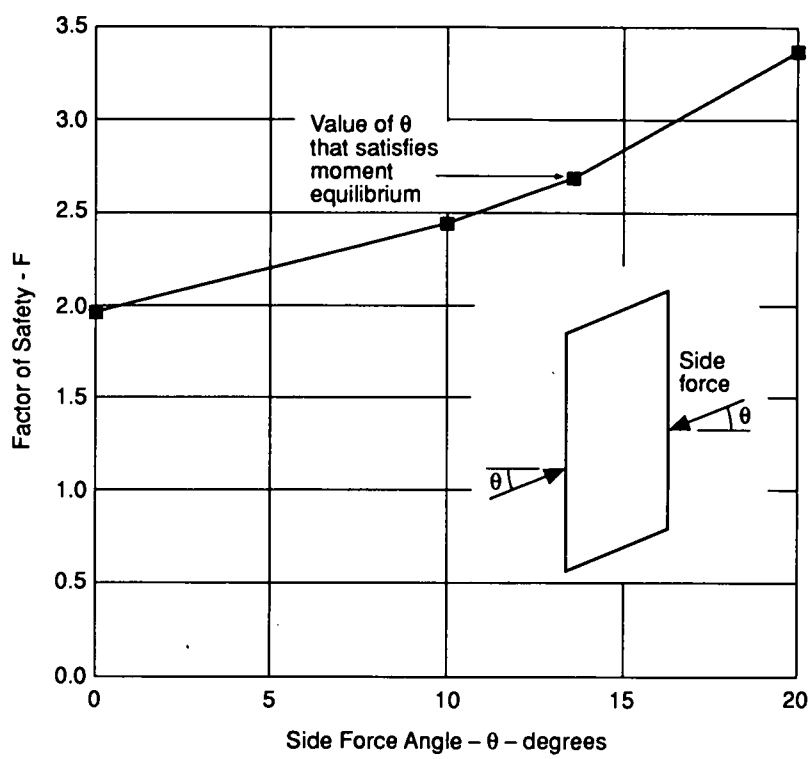

FIGURE 13-18
Variation of *F* with side force inclination assumed in force equilibrium analyses of sand embankment on clay.

6.2.2 Example Computer Analyses

A cross section through Waco Dam, in Texas, is shown in Figure 13-19. When the embankment

reached the height shown, a slide took place on the downstream slope (Wright and Duncan 1972). The key to the occurrence of the slide was the low undrained shear strength of the Pepper Shale (member of the Woodbine Formation) in the foundation. As shown in Figure 13-19(*a*), the Pepper Shale is highly anisotropic with respect to shear strength. The undrained strength on a horizontal plane (which was measured in laboratory tests using specimens trimmed so that their axes were 30 to 45 degrees from horizontal) was only about 40 percent of the strength measured on conventional vertical test specimens.

The rupture surface of the slide was located in the field by observation of the slide scarp and toe bulge and by inclinometers installed through the slide mass. As a result of the highly anisotropic strength of the Pepper Shale, the slip surface extended horizontally for a considerable distance downstream.

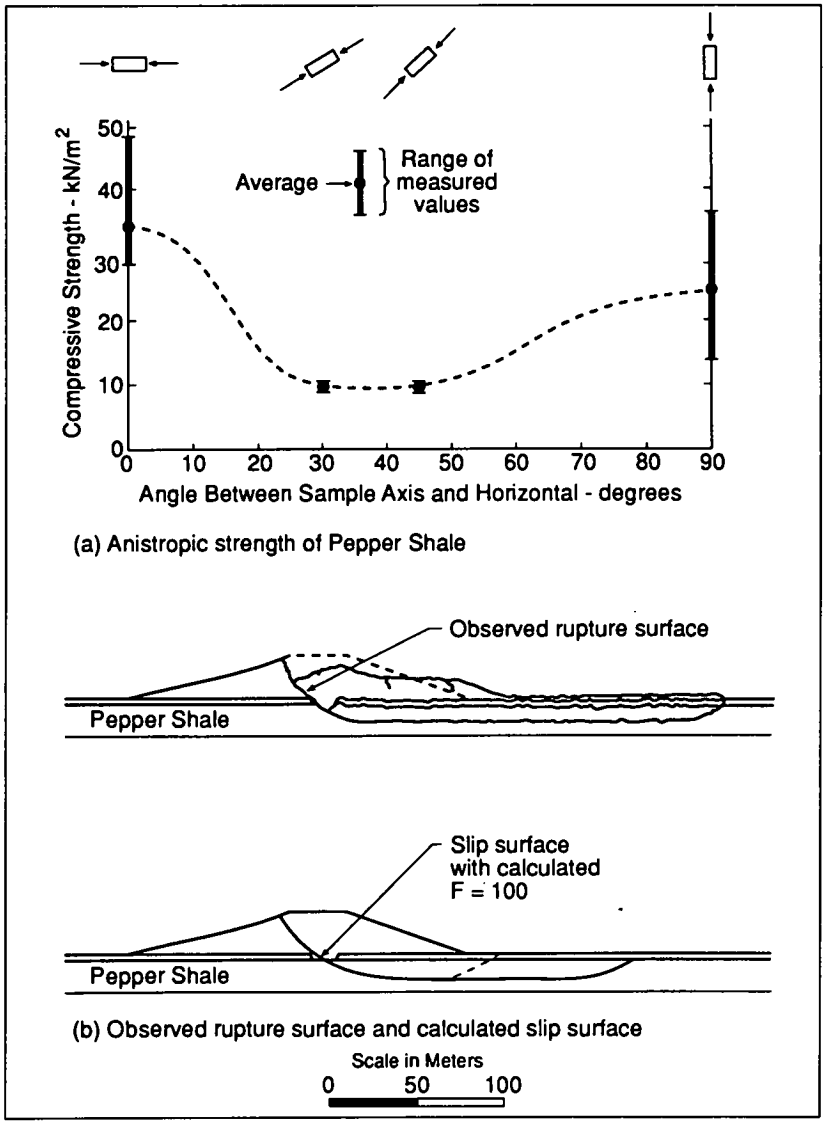

FIGURE 13-19 Analysis of slide in Waco Dam, Texas.

Postfailure analyses of this slide were complicated by two factors: (*a*) the anisotropic strength of the foundation soil and (*b*) the noncircular slip surface. As a result, it was not practical to perform postfailure analyses by hand. With a computer program using Spencer's method, a wide variety of analyses were performed to examine the correspondence among the observed slide, the shear strengths measured in the laboratory, and the most critical slip surface determined by analysis. As shown in Figure 13-19(*b*), the calculated slip surface for F = 1.00 was quite similar to the observed slip surface.

A cross section through the Cucaracha landslide at the Panama Canal is shown in Figure 13-20. This slope, which had suffered landslides during excavation of the canal, suffered another slide in 1986 (Berman 1988). The slip surface shown in Figure 13-20 was estimated on the basis of surface observations and inclinometer measurements.

The slide was caused by changes in the groundwater level, with perhaps some influence of loading at the top of the slope, at a location away from the section shown in Figure 13-20. Because the slide was caused by changes in the seepage conditions that resulted in increased pore pressures, it was a drained failure. Therefore the postfailure analyses were performed using drained strengths and the piezometric level that was estimated for the time of the failure.

The slide movement appeared to coincide with bedding surfaces in the Cucaracha shale, which contains numerous slickensides. It therefore seemed appropriate to use residual shear strengths on these bedding surfaces. The residual drained shear strength along the bedding is shown by the lower of the two strength envelopes in Figure 13-20(*a*). The shear strengths on surfaces cutting across bedding were found to be considerably higher, as shown by the upper curve in Figure 13-20(*a*).

The strength envelopes for shear along and across the bedding are nonlinear, and they cannot be represented accurately by single values of c and ϕ. Therefore, each strength envelope was represented by a series of points without reference to values of c and ϕ.

Postfailure analyses of the 1986 Cucaracha landslide involved a number of complications: noncir-

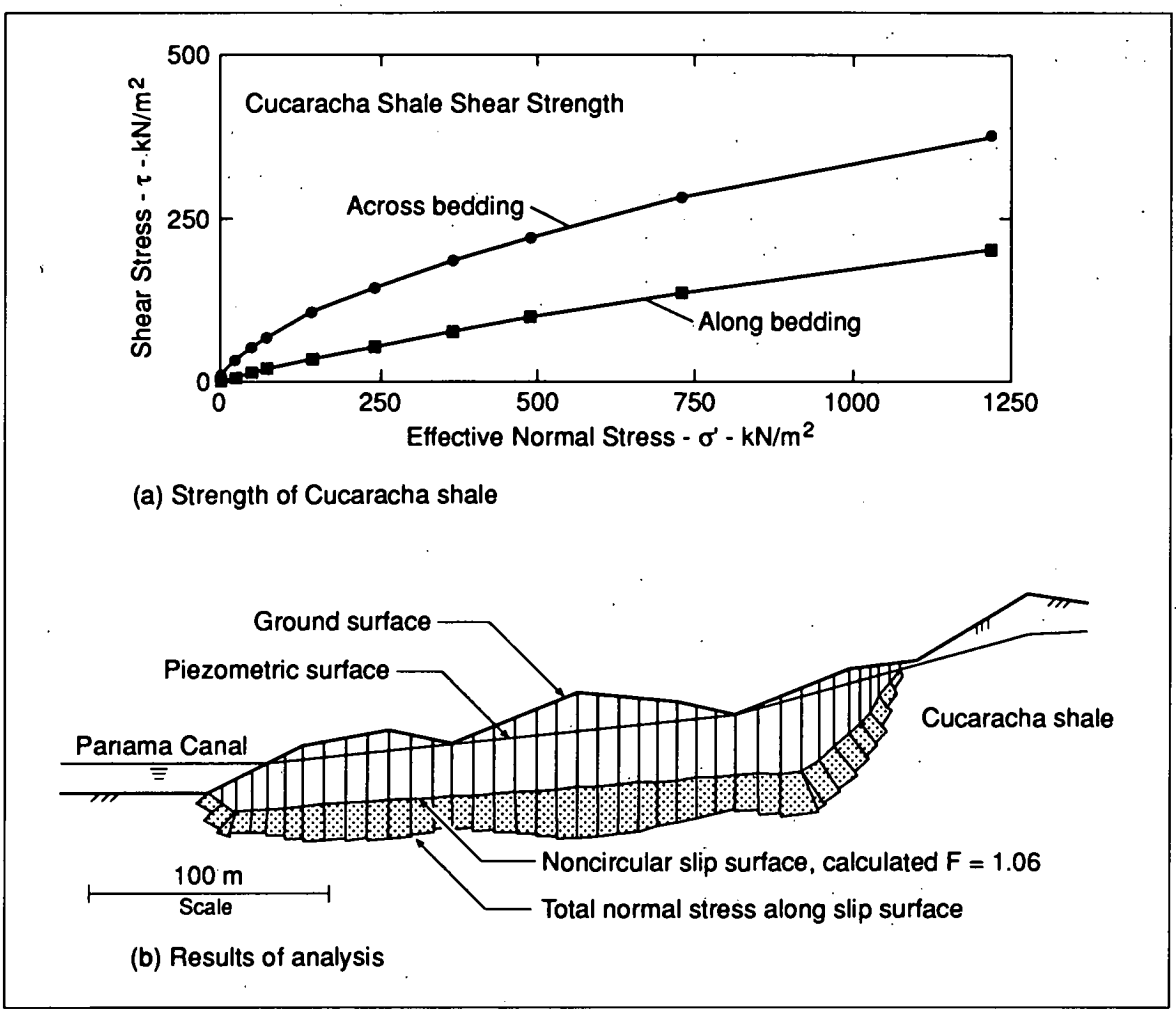

FIGURE 13-20 Analysis of 1986 Cucaracha landslide at Panama Canal.

cular slip surfaces, nonlinear shear strength envelopes, and shear strengths that varied with the orientation of the slip surface. Thorough computer analyses of the slide were performed, confirming the applicability of the shear strengths, and other analyses were made to evaluate the effectiveness of repair schemes (Berman 1988). The results of one of these analyses are shown in Figure 13-20(*b*).

6.2.3 Benefits and Risks of Computer Analyses

Computers afford the most effective means of analysis of slope stability in soil. Computer analyses can be accomplished quickly when a suitable computer program is available; they can accommodate complex conditions of site geometry, seepage, and shear strength; they can be performed using advanced methods that satisfy all conditions of equilibrium; and they can be used to perform thorough analyses to locate the critical slip surface. However, it should be borne in mind that a computer can also propagate mistakes much faster than is possible by hand. Computer analysis must be checked and verified before the results can be relied upon. Analyses can be checked using charts, manual calculations for the critical slip surface, and independent analysis with another computer program using independent input. Common sense and judgment must always be used to ensure that analysis conditions and results are reasonable.

7. BACK ANALYSIS TO DETERMINE SOIL STRENGTHS

The strength properties of many types of natural soil are difficult to determine reliably by means of laboratory tests. In cases where a landslide has

occurred and repair measures are being evaluated, it is often most effective to determine soil strength by back analysis. This process involves three steps:

1. The best estimates possible must be made of the soil strengths and unit weights using the information at hand. Laboratory tests and strength correlations provide an effective basis for these estimates. The slope geometry and phreatic conditions at the time of failure must also be established.
2. The slide should be analyzed using the estimated properties. If the calculated factor of safety is equal to 1.00, the properties and conditions represent a reasonable model of the slide. If the calculated factor of safety is not equal to 1.00, the strengths are adjusted until $F = 1.00$. The adjustment ratio need not be the same for all soils involved in the slide. Logically, larger adjustments should be made for strengths that are considered to involve greater degrees of uncertainty.
3. When values of soil strength have been determined that give $F = 1.00$ for the conditions at the time of failure, these strengths are used to evaluate repair measures.

This process was used to develop mitigative schemes for the Waco Dam slide discussed previously (Figure 13-19) and the 1986 Cucaracha landslide (Figure 13-20). A further example of back analysis is shown by the Olmsted landslide on the Illinois shore of the Ohio River (Filz et al. 1992).

A cross section through the Olmsted landslide is shown in Figure 13-21. The slide occurred on June 4, 1988, when the river dropped to a low level. The location of the rupture surface was known from

			ϕ'_r (degrees)		
Soil	Unit weight (kN/m³)	Plasticity Index	Lab tests	Correlations	Trial values
Alluvium	18.4	20 to 30	22 to 33	14 to 20	18
Colluvium	17.6	20 to 35	20 to 35	12 to 20	15
McNairy I	18.6	10 to 50	7 to 21	10 to 30	10 and 11 on bedding 25 across bedding
Potter's Creek	16.5	50 to 80	5 to 12	6 to 10	8

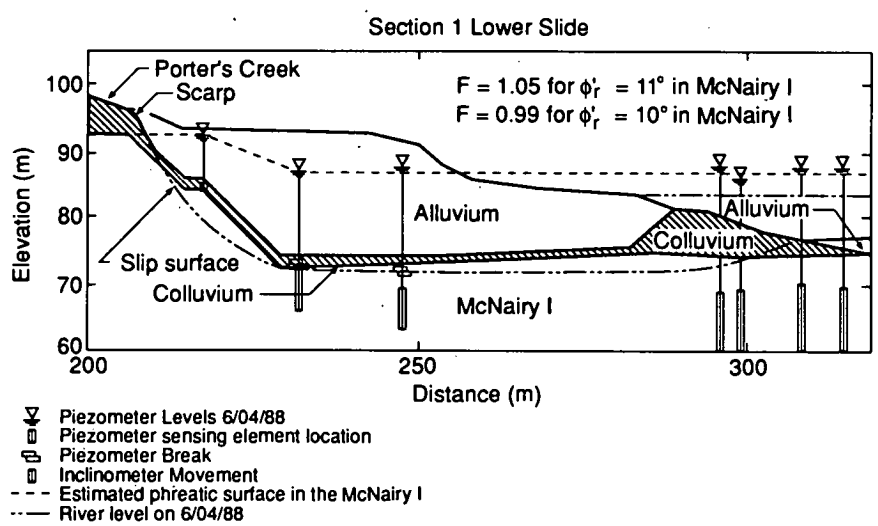

FIGURE 13-21
Back analysis of Olmsted landslide, Illinois.

the position of the scarp at the top of the slide, from movements in inclinometers installed after the slide, and from locations of breaks in piezometer riser tubes. Over most of its length, the rupture surface passed through the McNairy I formation, a sedimentary deposit of flat-lying interbedded sands and clays. The thickness of the individual layers ranged from a few millimeters to nearly a meter.

Laboratory tests were performed on all of the soils involved in the slide, with the results shown in the table at the top of Figure 13-21. It can be seen that there is considerable scatter in the results for all of the soils owing to the variability of the materials, the difficulties involved in obtaining representative and undisturbed specimens for testing, and the layering in McNairy I. On the basis of the results of the tests and correlations with plasticity index, trial values of residual friction angle were established for all of the soils. These are shown in the last column of the table.

The first analysis was performed using Spencer's method with ϕ'_r = 11 degrees in the McNairy I formation. The calculated factor of safety was 1.05. A second analysis, using ϕ'_r = 10 degrees, gave F = 0.99. Only the value of ϕ'_r for McNairy I was changed for the second analysis because it was considered to have the greatest effect on the results and was therefore the most important parameter in the analyses. The same strength parameter values were also used to analyze four other sections through the slide, where the geometry and piezometric levels were different. The calculated values of F, with ϕ'_r = 10 degrees in McNairy I, varied from 0.96 to 1.00 for the five sections. The parameters calculated by back analysis were considered to represent the behavior of the soils quite well and were utilized to analyze the effects of drainage and slope flattening to improve the stability of the slide area.

8. RAPID DRAWDOWN ANALYSIS

When the water level in a lake or stream adjacent to a slope drops, the stabilizing influence of the water pressure on the slope is lost. Many failures of dam slopes and submerged natural slopes have occurred during rapid drawdown. Analysis of rapid drawdown is therefore an important consideration for design of dams and other slopes that will be submerged and subject to such changes in water level.

Methods of analysis of stability during rapid drawdown have been evaluated by Duncan et al. (1990). On the basis of those studies, a method of analysis for rapid drawdown was developed that incorporates these features:

- Undrained strengths are used for soil zones that have values of C_v so low that they are unable to drain during the period of drawdown. Criteria to determine whether a soil zone is drained or undrained are described in Section 3.
- Analyses are performed in three steps:
  - Anisotropic consolidation pressures are determined for each slice using stability and seepage analyses for the predrawdown steady seepage conditions.
  - Values of undrained strength are determined for each slice with its base in a zone of soil that will be undrained, drained strengths are determined for zones of soil that will be drained, and an analysis of stability after drawdown using these strengths is performed.
  - The after-drawdown analyses are repeated using drained strengths for slices where the drained strengths after drawdown are found to be smaller than the undrained strengths.

Thus, the method uses drained or undrained strengths, whichever are lower, for slices where drainage is not expected during drawdown. This technique ensures that the method will not yield unconservative results if the soil drains faster than anticipated.

This method of analysis is logical in its treatment of strengths and stability. Used with Spencer's method for stability computations, it was found to give satisfactory results for Walter Bouldin Dam in Alabama and Pilarcitos Dam in California, both of which suffered embankment slides during rapid drawdown (Duncan et al. 1990).

9. ANALYSIS OF REINFORCED SLOPES

Reinforcing materials, such as geotextiles, geogrids, and steel grids, are widely used to strengthen slopes. Considerable research has been done to evaluate the long-term behavior of these materials and to investigate the mechanisms of interaction by which they improve the stability of slopes. The principal mechanism of reinforcement is limitation of tensile strains at the locations of the reinforcement. Reinforcing materials are commonly placed horizontally within the soil.

Studies of soil reinforcement have shown that the stability of reinforced slopes can be analyzed using the following simple procedure:

1. The long-term ultimate strength of the reinforcing material is determined. This determination involves consideration of short-term strength, creep under load, and the allowable tensile strains considering the type of slope or embankment and the sensitivity of the underlying foundation soil. This long-term limit load is expressed in units of force per unit length of the reinforcement.
2. The long-term limit load is divided by a reinforcement factor of safety, F_R, to produce a factored limit load. The value of F_R logically should depend on the reliability with which the limit load can be evaluated and the possible consequences of failure. Values of F_R near 1.5 are suitable for normal conditions.
3. The factored limit loads are used as known values in conventional limit equilibrium analyses of slope stability. The forces are applied to the bases of slices in which a potential slip surface cuts across the reinforcement. Studies have shown that very flexible types of reinforcement may be reoriented if slip occurs and dragged down so that they parallel the slip surface where they cross it. If a method of analysis is used that satisfies all conditions of equilibrium, the orientation of the reinforcement force (horizontal or parallel to the slip surface) has essentially no effect on the factor of safety computed (Wright and Duncan 1991). The factor of safety computed in this type of analysis is the same as that discussed earlier in this chapter; it is the factor by which the soil strength would have to be divided to bring the soil into a state of barely stable equilibrium.

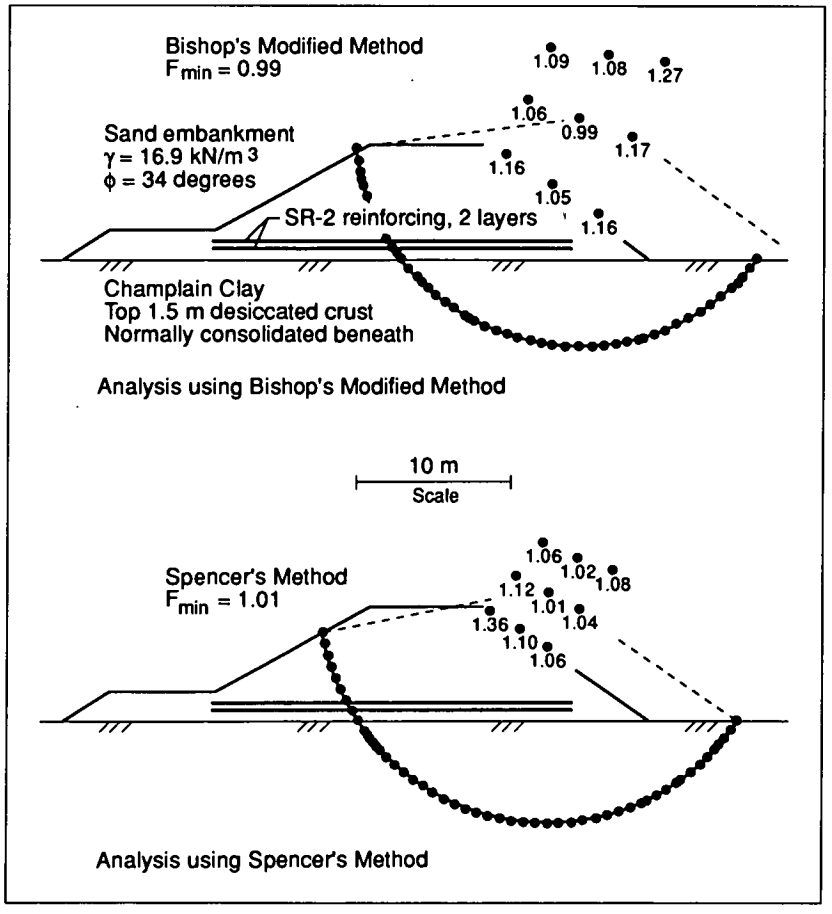

FIGURE 13-22
Analysis of reinforced St. Alban test embankment.

An example analysis of a reinforced slope is shown in Figure 13-22, in which cross sections through the St. Alban test embankment are used; this embankment was constructed on the sensitive Champlain Clay (Schaefer and Duncan 1988). To avoid uncertainties resulting from the sensitivity of the clay, the analyses described here were performed using the postpeak residual undrained shear strength of the crust and the normally consolidated clay beneath the crust. As defined by La Rochelle et al. (1974) and Trak et al. (1980), this "residual" undrained strength is measured at 15 percent axial strain in triaxial tests and is equal to about 90 percent of the undrained strength measured in field vane-shear tests.

The sand embankment was reinforced with two horizontal layers of Tensar SR-2 geogrid. Failure took place as the embankment was being raised about 20 days after construction began. For this load duration, the limit load corresponding to 10 percent strain is about 32 kN/m. Analyses were performed at this reinforcement magnitude using Bishop's modified method and Spencer's method. The results of the analyses are shown in Figure 13-22.

In both analyses the reinforcement force was assumed to act horizontally. It can be seen that both analyses resulted in minimum factors of safety very close to unity. For practical purposes, the values of F calculated by the two analyses were the same. Considering the arbitrary choice of 10 percent strain as the failure strain in the reinforcing, the fact that the calculated factors of safety were so close to unity must be considered somewhat fortuitous.

10. THREE-DIMENSIONAL ANALYSES OF SLOPE STABILITY

Although the methods of slope stability analyses discussed in the previous sections are formulated in two dimensions, actual slope failures are three-dimensional. The question therefore arises as to the accuracy and reliability of two-dimensional (2D) analyses applied to three-dimensional (3D) problems. Research studies [for example, the work by Cavounidis (1987)] have shown clearly that factors of safety calculated using 3D analyses are larger than those calculated using 2D analyses, all other things being equal. Implicit in this conclusion is the notion that the 2D section analyzed is the most critical section through the 3D potential sliding mass.

An example is shown in Figure 13-23, which summarizes 2D and 3D analyses of an ellipsoidal slip surface (Hungr et al. 1989). As shown in Figure 13-23(*a*), the factors of safety for three 2D sections through the sliding mass are F_2 = 1.10, 1.00, and 1.19. The central section (Section 2) is the most critical, and the minimum 2D factor of safety is thus the value calculated for this section, F_2 = 1.00. Figure 13-23(*b*) shows the results of a 3D analysis performed by Hungr et al. (1989) using Bishop's modified method extended to three dimensions (Hungr 1987). The shape of the critical ellipsoidal slip surface is shown in Figure 13-23(*c*). The minimum 3D factor of safety for this case is F_3 = 1.01, which is only 1.0 percent higher than the minimum 2D factor of safety.

It is more difficult to perform 3D analyses than 2D analyses. Because 2D analyses give somewhat conservative results ($F_2 \leq F_3$, all other things being equal), they provide a reasonable and sufficiently accurate approach to most practical problems of stability of soil slopes. Use of 2D analyses requires that the section or sections analyzed be selected using judgment regarding which section will be most critical. In many cases, as in that shown in

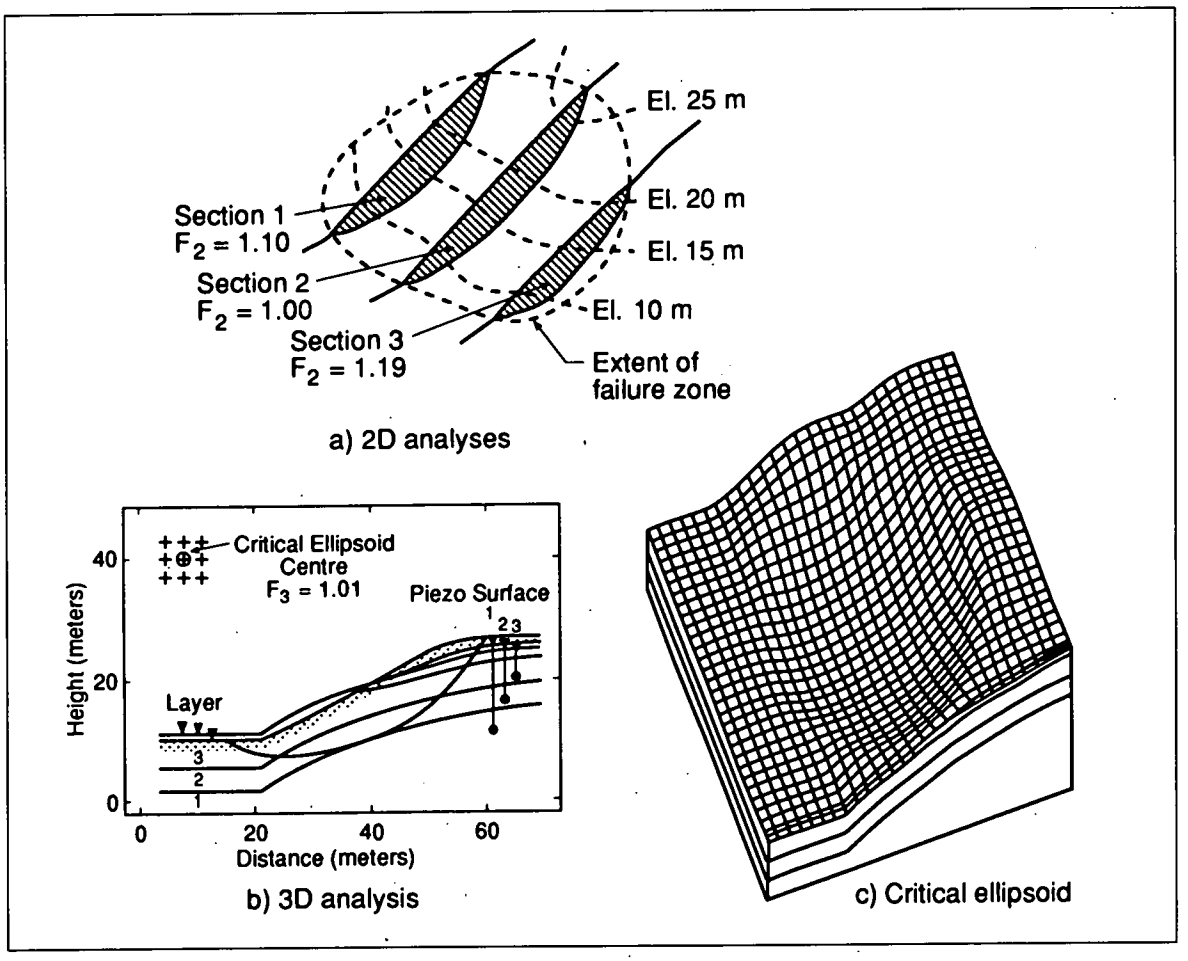

FIGURE 13-23 Comparison of two-dimensional and three-dimensional analyses.

Figure 13-23, the critical 2D section is the one where the slip surface can cut most deeply. In some cases other sections may be more critical. If there is doubt concerning which 2D section is most critical, several should be analyzed.

11. DEFORMATION ANALYSIS

Finite-element analyses have been used since the mid-1960s for analysis of stresses and movements in slopes. A recent review (Duncan 1992) described more than 100 examples of their application. Even though finite-element analyses have been used fairly often in recent years for evaluation of slope deformations, the procedure is not routine. Finite-element analyses are more difficult and time-consuming than slope stability analyses, and they require special expertise if they are to be done successfully and productively.

Experience with finite-element analyses has shown that they are most useful when performed in conjunction with field instrumentation studies. They can be valuable in planning instrumentation programs by showing where the largest movements would be expected to occur and how large they may be. They can also be used for interpreting the results of instrumentation studies. If calculated and measured movements are in agreement at the locations of the instruments, this suggests that the analytical results also may provide reasonable indications of behavior at other locations. Often the more complete finite-element results provide insight into the causes and significance of the measured movements.

An example of a finite-element analysis, summarized in Figure 13-24, concerns Otter Brook Dam in New Hampshire, which deformed considerably during construction (Kulhawy et al. 1969). The embankment, about 40 m high, is essentially homogeneous. It was constructed of compacted silt on a firm foundation of glacial till over rock.

As shown in Figure 13-24, a bridge pier was constructed at about mid-height on the upstream slope of the dam. Because the embankment was constructed above the level of the bridge pier, the embankment deformed under the weight of the added material and the lower part bulged outward. Measurements were made of the movements of the bridge pier as the embankment was constructed. As shown in Figure 13-24(*c*), these measurements reached about 0.15 m vertically and about 0.9 m horizontally by the end of construction. Measurements at other elevations on the upstream slope, also shown in Figure 13-24(*c*), showed that the maximum horizontal movement occurred near mid-height of the embankment.

A finite-element analysis of Otter Brook Dam was performed by Kulhawy et al. (1969) using hyperbolic stress-strain properties determined from conventional laboratory tests. The tests had been performed in support of stability analyses of the dam. The calculated displacements of the upstream slope and the bridge pier are compared with the measured values in Figure 13-24(*c*). It can be seen that agreement is quite good, indicating that the finite-element analyses afford a reasonable representation of the actual behavior of the embankment.

Because engineered fills are water conditioned and compacted with a reasonable degree of control of density and uniformity of the fill, stress-strain properties can be determined for these materials more precisely than for natural soil deposits, which may be less uniform and may have more complex behavior. As a result, the reliability of calculated movements is not as great for natural soil deposits as for embankments. Very often, even in the case of embankments, the agreement between calculated and measured movements is not as close as that shown in Figure 13-24.

12. USE OF CENTRIFUGE EXPERIMENTS

Centrifuge experiments have been used to study problems of slope stability and deformation behavior since the early 1970s (Schofield 1980). Techniques have been developed for constructing model slopes, varying water levels, measuring shear strengths, and measuring displacements in the models while they are rotating. The techniques were applied to studies of levee failures (Kusakabe et al. 1988), highway embankment settlement and stability (Feng and Hu 1988), settlement and cracking in dams (Shcherbina and Olympiev 1991; Zhang and Hu 1991; Zhu et al. 1991), stability of tailings dams (Liu et al. 1988), mechanisms of flow slides (Schofield 1980), and stabilization of slopes by drainage (Resnick and Znidarcic 1990).

The method has the greatest value for qualitative studies of mechanisms of deformation and failure. Because centrifuge models can be constructed so that they simulate the geometry and

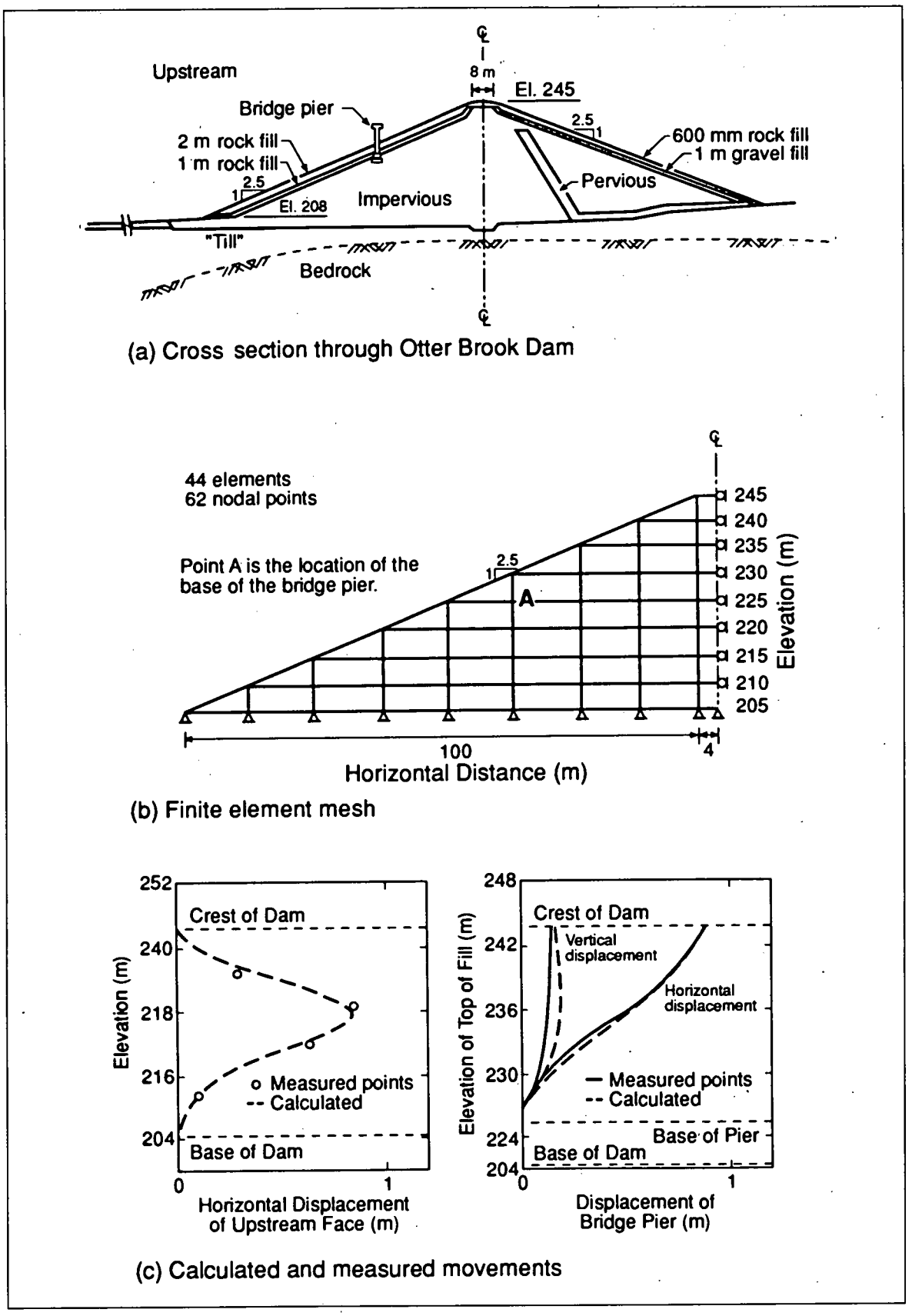

FIGURE 13-24 Finite-element analysis of Otter Brook Dam, New Hampshire.

stresses in prototype slopes, they are capable, in principle, of simulating the modes of deformation and failure to be expected in the field. Thus, they are useful where mechanisms of deformation and failure are unknown.

Limitations on the use of centrifuge experiments to derive quantitative results stem from the difficulties inherent in constructing centrifuge models that accurately mimic the important details of the full-scale prototype and the loading conditions it will experience. These difficulties, plus the fact that the technique is costly and requires highly specialized equipment, appear to be the principal limitations on its use for practical studies of stability and deformation in soil slopes.

REFERENCES

Berman, G. 1988. *Landslide Control on the Panama Canal: Status Report—1988*. Geotechnical Branch, Engineering Division, Panama Canal Commission, Panama City, 26 pp.

Bishop, A. W. 1955. The Use of the Slip Circle in the Stability Analysis of Slopes. *Geotechnique*, Vol. 5, No. 1, pp. 7–17.

Bishop, A. W., and L. Bjerrum. 1960. The Relevance of the Triaxial Test to the Solution of Stability Problems. In *Proc., ASCE Research Conference on the Shear Strength of Cohesive Soils*, Boulder, Colorado, American Society of Civil Engineers, New York, pp. 437–501.

Cavounidis, S. 1987. On the Ratio of Factors of Safety in Slope Stability Analyses. *Geotechnique*, Vol. 37, No. 2, pp. 207–210.

Duncan, J. M. 1992. State-of-the-Art: Static Stability and Deformation Analysis. In *Proc., ASCE Specialty Conference on Stability and Performance of Slopes and Embankments II*, Berkeley, California, Geotechnical Special Publication 31, American Society of Civil Engineers, New York.

Duncan, J. M., A. L. Buchignani, and M. De Wet. 1987. *An Engineering Manual for Slope Stability Studies*. Virginia Polytechnic Institute and State University, Blacksburg, 80 pp.

Duncan, J. M., S. G. Wright, and K. S. Wong. 1990. Slope Stability During Rapid Drawdown. In *Proc., H. Bolton Seed Memorial Symposium*, Berkeley, California, Bitech Publishers, Vancouver, British Columbia, Canada.

Fellenius, W. 1927. *Erdstatische Berechnungen mit Reibung und Kohasion*. Ernst, Berlin.

Feng, G., and Y. Hu. 1988. Centrifugal Model Test of a Highway Embankment on Soft Clay. In *Proc., First International Conference on Geotechnical Centrifuge Modeling*, Paris, pp. 153–162.

Filz, G. M., T. L. Brandon, and J. M. Duncan. 1992. Back Analysis of the Olmsted Landslide Using Anisotropic Strengths. In *Transportation Research Record 1343*, TRB, National Research Council, Washington, D.C., pp. 72–78.

Hungr, O. 1987. An Extension of Bishop's Simplified Method of Slope Stability Analysis to Three Dimensions. *Geotechnique*, Vol. 37, No. 1, pp. 113–117.

Hungr, O., F. M. Salgado, and P. M. Byrne. 1989. Evaluation of a Three-Dimensional Method of Slope Stability Analysis. *Canadian Geotechnical Journal*, Vol. 26, pp. 679–686.

Hunter, J. H., and R. L. Schuster. 1968. Stability of Simple Cuttings in Normally Consolidated Clays. *Geotechnique*, Vol. 18, No. 3, pp. 372–378.

Janbu, N. 1968. *Slope Stability Computations*. Soil Mechanics and Foundation Engineering Report. Technical University of Norway, Trondheim.

Kulhawy, F. H., J. M. Duncan, and H. B. Seed. 1969. *Finite Element Analyses of Stresses and Movements in Embankments During Construction*. Report TE 69-4. Office of Research Services, University of California, 169 pp.

Kusakabe, O., A. Kawashima, and T. Hagiwara. 1988. Levee Failures Modeled in Drum Centrifuge. In *Proc., First International Conference on Geotechnical Centrifuge Modeling*, Paris, pp. 147–152.

Ladd, C. C., and R. Foott. 1974. New Design Procedure for Stability of Soft Clays. *Journal of the Geotechnical Engineering Division*, ASCE, Vol. 100, No. 7, pp. 763–786.

LaRochelle, P., B. Trak, F. Tavenas, and M. Roy. 1974. Failure of a Test Embankment on a Sensitive Champlain Clay Deposit. *Canadian Geotechnical Journal*, Vol. 11, No. 1, pp. 142–164.

Liu, L., W. Jiang, and W. Han. 1988. Centrifugal Model Tests for Stability of Ash Soil Composite Dams. In *Proc., First International Conference on Geotechnical Centrifuge Modeling*, Paris, pp. 141–146.

Lowe, J., and L. Karafiath. 1960. Stability of Earth Dams upon Drawdown. In *Proc., First Pan-American Conference on Soil Mechanics and Foundation Engineering*, Mexico City, Vol. 2, pp. 537–552.

Morgenstern, N. R. 1992. The Evaluation of Slope Stability—A 25 Year Perspective. In *Proc., ASCE Specialty Conference on Stability and Performance of Slopes and Embankments II*, Berkeley, California,

Geotechnical Special Publication 31, American Society of Civil Engineers, New York, pp. 1–26.

Morgenstern, N. R., and V. E. Price. 1965. The Analysis of the Stability of General Slip Surfaces. *Geotechnique*, Vol. 15, No. 1, pp. 79–93.

Resnick, G. S., and D. Znidarcic. 1990. Centrifugal Modeling of Drains for Slope Stabilization. *Journal of Geotechnical Engineering*, ASCE, Vol. 116, No. 11, pp. 1607–1624.

Sarma, S. K. 1973. Stability Analysis of Embankments and Slopes. *Geotechnique*, Vol. 23, pp. 423–433.

Schaefer, V. R., and J. M. Duncan. 1988. Finite Element Analyses of the St. Alban Test Embankments. In *Proc., Symposium on Geosynthetics for Soil Improvement*, National Convention, Nashville, American Society of Civil Engineers, pp. 158–177.

Schofield, A. N. 1980. Cambridge Geotechnical Centrifuge Operations. *Geotechnique*, Vol. 30, No. 3, pp. 227–268.

Shcherbina, V. I., and D. N. Olympiev. 1991. Numerical and Centrifugal Modeling of Cracking in an Earth-and-Rockfill Dam Core. In *Proc., Second International Conference on Geotechnical Centrifuge Modeling*, Boulder, Colorado, pp. 67–74.

Skempton, A. W. 1970. First-Time Slides in Overconsolidated Clays. *Geotechnique*, Vol. 20, No. 4, pp. 320–324.

Skempton, A. W. 1977. Slope Stability of Cuttings in London Clay. In *Proc., Ninth International Conference on Soil Mechanics and Foundation Engineering*, Tokyo, pp. 261–270.

Skempton, A. W. 1985. Residual Strength of Clays in Landslides, Folded Strata, and the Laboratory. *Geotechnique*, Vol. 35, No. 1, pp. 3–18.

Spencer, E. 1967. A Method of Analysis of the Stability of Embankments Assuming Parallel Interslice Forces. *Geotechnique*, Vol. 17, No. 1, pp. 11–26.

Trak, B., P. LaRochelle, F. Tavenas, S. Leroueil, and M. Roy. 1980. A New Approach to the Stability Analysis of Embankments on Sensitive Clays. *Canadian Geotechnical Journal*, Vol. 17, No. 4, pp. 526–584.

U.S. Army Corps of Engineers. 1970. *Engineering and Design—Stability of Earth and Rockfill Dams*. Engineer Manual EM 1110-2-1902. Department of the Army, Corps of Engineers, Office of the Chief of Engineers, Washington, D.C.

Wright, S. G., and J. M. Duncan. 1972. Analysis of Waco Dam Slide. *Journal of the Soil Mechanics and Foundations Division*, ASCE, Vol. 98, No. SM7, pp. 653–665.

Wright, S. G., and J. M. Duncan. 1991. Limit Equilibrium Stability Analyses for Reinforced Slopes. In *Transportation Research Record 1330*, TRB, National Research Council, Washington, D.C., 1991, pp. 40–46.

Zhang, L., and T. Hu. 1991. Centrifugal Modeling of the Pubugan High-Rise Rockfill Dam. In *Proc., Second International Conference on Geotechnical Centrifuge Modeling*, Boulder, Colorado, pp. 45–50.

Zhu, W., J. Yi, D. Zhu, and S. Liu. 1991. Application of Centrifuge Modeling to Predictions of Earth-Rockfill Dam Core Cracking. In *Proc., Second International Conference on Geotechnical Centrifuge Modeling*, Boulder, Colorado, pp. 59–66.